

EXPERIMENTAL AND ANALYTICAL STUDY ON TORSIONAL BEHAVIOR OF RC FLANGED BEAMS STRENGTHENED WITH GLASS FRP

NAVEEN SURE



**Department of Civil Engineering
National Institute of Technology, Rourkela
Rourkela-769 008, Odisha, India**

EXPERIMENTAL AND ANALYTICAL STUDY ON TORSIONAL BEHAVIOR OF RC FLANGED BEAMS STRENGTHENED WITH GLASS FRP

A THESIS SUBMITTED IN PARTIAL FULFILMENT
OF THE REQUIREMENTS FOR THE DEGREE OF

Master of Technology

in

Structural Engineering

by

NAVEEN SURE

(Roll No. 211CE2239)



**DEPARTMENT OF CIVIL ENGINEERING
NATIONAL INSTITUTE OF TECHNOLOGY, ROURKELA
ROURKELA – 769 008, ODISHA, INDIA
January 2013**

EXPERIMENTAL AND ANALYTICAL STUDY ON TORSIONAL BEHAVIOR OF RC FLANGED BEAMS STRENGTHENED WITH GLASS FRP

*A THESIS SUBMITTED IN PARTIAL FULFILMENT
OF THE REQUIREMENTS FOR THE DEGREE OF*

**Master of Technology
in
Structural Engineering**

by

NAVEEN SURE

Under the guidance of

Prof. A.PATEL



**DEPARTMENT OF CIVIL ENGINEERING
NATIONAL INSTITUTE OF TECHNOLOGY, ROURKELA
ROURKELA – 769 008, ODISHA, INDIA
JUNE 2013**



Department of Civil Engineering
National Institute of Technology, Rourkela
Rourkela – 769 008, Odisha, India

CERTIFICATE

*This is to certify that the thesis entitled, “**EXPERIMENTAL AND ANALYTICAL STUDY ON TORSIONAL BEHAVIOR OF RC FLANGED BEAMS STRENGTHENED WITH GLASS FRP**” submitted by **NAVEEN SURE** bearing Roll No. **211CE2239** in partial fulfilment of the requirements for the award of **Master of Technology Degree in Civil Engineering** with specialization in “**Structural Engineering**” during 2012-13 session at National Institute of Technology, Rourkela is an authentic work carried out by her under our supervision and guidance.*

To the best of our knowledge, the matter embodied in the thesis has not been submitted to any other University/Institute for the award of any Degree or Diploma.

Prof. A .PATEL

Date:

Place:Rourkela

ABSTRACT

Environmental degradation, increased service loads, reduced capacity due to aging, degradation owing to poor construction materials and workmanships and conditional need for seismic retrofitting have demanded the necessity for repair and rehabilitation of existing structures. Fibre reinforced polymers has been used successfully in many such applications for reasons like low weight, high strength and durability. Many previous research works on torsional strengthening were focused on solid rectangular RC beams with different strip layouts and different types of fibres. Various analytical models were developed to predict torsional behavior of strengthened rectangular beams and successfully used for validation of the experimental works. But literature on torsional strengthening of RC T- beam is limited.

In the present work experimental study was conducted in order to have a better understanding the behavior of torsional strengthening of solid RC flanged T-beams. An RC T-beam is analyzed and designed for torsion like an RC rectangular beam; the effect of concrete on flange is neglected by codes. In the present study effect of flange part in resisting torsion is studied by changing flange width of controlled beams. The other parameters studied are strengthening configurations and fiber orientations.

The objective of present study is to evaluate the effectiveness of the use of epoxy-bonded GFRP fabrics as external transverse reinforced to reinforced concrete beams with flanged cross sections (T-beam) subjected to torsion. Torsional results from strengthened beams are compared with the experimental result of the control beams without FRP application. The study shows remarkable improvement in torsional behavior of all the GFRP strengthen beams. The experimentally obtained results are validated with analytical model presented by A.Deifalla and A. Ghobarah and found in good agreement.

ACKNOWLEDGEMENT

The satisfaction and euphoria on the successful completion of any task would be incomplete without the mention of the people who made it possible whose constant guidance and encouragement crowned out effort with success.

I would like to express my heartfelt gratitude to my esteemed supervisor, Prof. A.Patel for his technical guidance, valuable suggestions, and encouragement throughout the experimental and theoretical study and in preparing this thesis. It has been an honour to work under Prof. A.Patel, whose expertise and discernment were key in the completion of this project.

I am grateful to the **Dept. of Civil Engineering, NIT ROURKELA**, for giving me the opportunity to execute this project, which is an integral part of the curriculum in M.Tech programme at the National Institute of Technology, Rourkela.

Many thanks to my friends who are directly or indirectly helped me in my project work for their generous contribution towards enriching the quality of the work. I would also express my obligations to Mr. S.K. Sethi, Mr. R. Lugun & Mr. Sushil, Laboratory team members of Department of Civil Engineering, NIT, Rourkela and academic staffs of this department for their extended cooperation.

This acknowledgement would not be complete without expressing my sincere gratitude to my parents for their love, patience, encouragement, and understanding which are the source of my motivation and inspiration throughout my work. Finally I would like to dedicate my work and this thesis to my parents.

NAVEEN SURE

TABLE OF CONTENT

	Page
ABSTRACT	i
ACKNOWLEDGMENTS	ii
LIST OF FIGURES	vii
LIST OF TABLES	xiii
NOTATIONSx
ACRONYMS AND ABBREVIATIONS	xi

CHAPTER 1 **INTRODUCTION**

1.1 overview	1
1.2 Torsional strenghtening of beams	3
1.3 Advantages and disadvantages of frp.....	4
1.3.1 Advantages.....	4
1.3.2 Disadvantages.....	5
1.4 Organization of thesis.....	5

CHAPTER 2 **REVIEW OF LITERATURE**

2.1 Brief Review	7
2.2 Literature review on torsional strengthening of RC beam.....	9
2.3 Critical observation from the literature.....	14
2.4 Objective and scope of the present work.....	15

CHAPTER 3 **EXPERIMENTAL PROGRAM**

3.1 casting of specimens.....	18
3.2 Material Properties	18

3.2.1 Concrete	18
3.2.2 Cement	20
3.2.3 Fine Aggregate	20
3.2.4 Coarse Aggregate	21
3.2.5 Water	21
3.2.6 Reinforcing Steel	21
3.3 Mixing of Concrete	22
3.3.1 Compaction	22
3.3.2 Curing of Concrete	23
3.4 Fiber Reinforced Polymer (FRP).....	23
3.4.1 Epoxy resin.....	23
3.4.2 Casting of GFRP Plate for tensile strength.....	24
3.4.3 Determination of Ultimate Stress, Ultimate Load & Young's Modulus of FRP.....	26
3.5 Strengthening of beams	28
3.6 Form work.....	30
3.7 Experimental setup.....	30
3.8 Description of specimens.....	32
3.8.1 Group-A.....	33
3.8.1.1 T-Beam(T2C).....	33

3.8.2 Group-B.....	33
3.8.2.1 Control Beam (T3C).....	33
3.8.2.2 Strengthened T- beam (T3SU).....	34
3.8.2.3 Strengthened T- beam (T3SUA).....	34
3.8.2.4 Strengthened T- beam (T3SF).....	35
3.8.2.5 Strengthened T- beam (T3S45).....	35
3.8.3 Group-C.....	36
3.8.3.1 T- beam (T4C).....	36
3.9 testing of beams.....	38
3.9.1 Beam (T2C).....	39
3.9.2 Beam (T3C).....	40
3.9.3 Beam (T4C).....	41
3.9.4 Beam (T3SU).....	42
3.9.5 Beam (T3SUA).....	44
3.9.6 Beam (T3SF).....	45
3.9.7 Beam (T3S45).....	47
3.9.8 Beam (T4SU).....	49

3.9.9 Beam (T4SUA).....	51
3.9.10 Beam (T4SF).....	53
3.9.11 Beam (T4S45).....	55
3.10 Summary.....	57

CHAPTER 4 TEST RESULTS & DISCUSSIONS

4.1 Experimental results.....	60
4.2 Failure Modes	60
4.3 Torsional moment and angle of twist analysis	61
4.3.1 Torsional moment and Angle of twist Analysis of all Beams.....	61
4.3.1.1 Control Beam (R1C).....	62
4.3.1.2 Beam (T2C).....	64
4.3.1.3 Beam (T3C).....	65
4.3.1.4 Beam (T3SU).....	66
4.3.1.5 Beam (T3SUA).....	68
4.3.1.6 Beam (T3SF).....	69
4.3.1.7 Beam (T3S45).....	71
4.3.1.8 Beam (T4C).....	73

4.3.1.9 Beam (T4SU).....	74
4.3.1.10 Beam (T4SUA).....	76
4.3.1.11 Beam (T4SF).....	78
4.3.1.12 Beam (T4S45).....	80
4.4 Torsional Moment vs. Angle of Twist Curves.....	81
<u>CHAPTER 5</u> ANALYTICAL ANALYSIS.....	86
<u>CHAPTER 6</u> CONCLUSIONS & RECOMMENDATIONS.....	90
<u>CHAPTER 7</u> REFERENCES	93

LIST OF FIGURES

Figure		Page
Chapter 3		
3-1.	Detailing of Reinforcement	22
3-2.	Specimens for tensile testing of woven Glass/Epoxy composite	25
3-3.	Experimental setup of INSTRON universal testing Machine (SATEC) of 600 kN capacity	26
3-4.	Specimen during testing	26
3-5.	Application of epoxy and hardener on the beam.....	29
3-6.	Roller used for the removal of air bubble.....	29
3-7.	Steel Frame Used For Casting of RC T-Beam.....	30
3-8.	Loading Setup.....	31
3-9.	Shear force and bending moment diagram for two point loading.....	32
3-10.	Model of T-beam without GFRP and 250mm width of Flange, Control Beam	33
3-11.	T-beam without GFRP and 350mm width of Flange, Control beam (T3C)	34
3-12.	T-beam Strengthened with GFRP of U-Wrap.....	34
3-13.	T-beam Strengthened with GFRP of U-Wrap with flange anchorage.....	35
3-14.	T-beam Strengthened with GFRP of fully wrapped beam.....	35
3-15.	T-beam Strengthened with GFRP strips wrapped with an inclination of 45°.....	36
3-16.	T-beam without GFRP and 450mm width of Flange, Control beam.....	36
3-17.	T-beam Strengthened with GFRP of U-Wrap.....	37
3-18.	T-beam Strengthened with GFRP of U-Wrap with flange anchorage.....	37
3-19.	T-beam Strengthened with GFRP of fully wrapped beam.....	37
3-20.	T-beam Strengthened with GFRP strips wrapped with an inclination of 45°.....	37
3-21.	Cracks pattern in beam.....	39
3-22.	cracks pattern in beam.....	40
3-23.	(a) Control Beam after cracking (T4C).....	41
	(b) Crack pattern at face-1.....	41
	(c) Crack pattern at face-2.....	41

3-24	(a) U- Wrapped beam after cracking.....	42
	(b) Closed view of cracks.....	43
	(c) Crack pattern in flange.....	43
3-25	(a) Experimental Setup of the U-Wrap with Anchorage system Beam No.6 (T3SUA).....	44
	(b) Closed view of Cracks.....	44
	(c) Cracks on Flange of Beam.....	44
3-26	(a) Fully Wrapped beam after Cracking.....	45
	(b) Cracks on Flange of Beam.....	46
	(c) Closed view of Cracks.....	46
3-27	(a) Beam wrapped with 100mm Bi-directional GFRP (45°) after cracking.....	47
	(b) Closed view of cracks.....	48
	(c) crack in the flange.....	48
3-28	(a) Beam 450mm flange strengthened with GFRP (U-Wrap).....	49
	(b) crack pattern at the main beam.....	49
	(b) Cracks in the flange portion.....	49
3-29	(a) Beam with U-wrap with flange anchorage system of GFRP (T4SUA).....	51
	(b) closed view of crack.....	51
	(c) closed view of crack.....	51
3-30	(a) Fully Wrapped beam after Cracking of 450mm wide flange.....	53
	(b) Debonding of FRP in web.....	53

	(c) Cracks in flange.....	53
3-31	(a) Cracks in the web portion for 45° wrapping.....	55
	(b) Debonding of FRP near the loading arm.....	55
	(c) Rupture in the GFRP.....	55

Chapter 4

4-1	(a) Experimental Setup of the Control Beam R1C.....	62
	(b) Crack pattern at face-1	62
	(c) crack pattern face-2	62
4-2	Torsional moment Vs Angle of Twist for Beam R1C.....	63
4-3	Cracks Pattern in T2C.....	64
4-4	Torsional moment Vs Angle of Twist for Beam T2C.....	65
4-5	Spiral crack in the beam.....	65
4-6	Torsional moment Vs Angle of Twist curve (T3C).....	66
4-7	(a) Initial hairline crack.....	67
	(b) Crack at ultimate load.....	67
4-8	Torsional moment Vs Angle of Twist curve (T3SU).....	67
4-9	(a) Closed view of Cracks.....	68
	(b) Cracks on Flange of Beam.....	68
4-10	Torsional moment Vs Angle of Twist curve (T3SUA).....	69
4-11	(a) Fully Wrapped beam after Cracking.....	69

	(b) Cracks on Flange of Beam.....	70
	(c) Closed view of Cracks.....	70
4-12	Torsional moment Vs Angle of Twist curve (T3SF).....	71
4-13	(a) Beam wrapped with 100mm Bi-directional GFRP (45°) after cracking.....	71
	(b) Closed view of cracks.....	72
	(c) crack in the flange.....	72
4-14	Torsional moment Vs Angle of Twist curve (T3S45).....	72
4-15	(a) Crack pattern at face-1.....	73
	(b) Crack pattern at face-2.....	73
4-16	Torsional moment Vs Angle of Twist curve (T3C).....	74
4-17	(a) Beam 450mm flange strengthened with GFRP (U-Wrap).....	74
	(b) Crack pattern at the main beam.....	75
	(c) Cracks in the flange portion.....	75
4-18	Torsional moment Vs Angle of Twist curve (T4SU).....	76
4-19	(a) a closed view of crack.....	76
	(b) Crack in web portion.....	76
4-20	Torsional moment Vs Angle of Twist curve (T4SUA).....	77
4-21	(a) Fully Wrapped beam after Cracking of 450mm wide flange.....	78
	(b) Debonding of FRP in web.....	79
	(c) cracks in flange.....	79

4-22	Torsional moment Vs Angle of Twist curve (T4SF).....	79
4-23	(a) cracks in the web portion for 45° wrapping.....	80
	(b) Debonding of FRP near the loading arms.....	81
4-24	Torsional moment Vs Angle of Twist curve (T4S45).....	81
4-25	Effect of GFRP Strengthened patterns for Series B beams.....	82
4-26	Effect of GFRP Strengthened patterns for Series C beams.....	83
4-27	Effect of flange width in control beams.....	84
4-28	Effect of GFRP Strengthened patterns for T3SU vs T4SU beams.....	84
4-29	Effect of GFRP Strengthened patterns for T3SUA vs T4SUA beams.....	85

LIST OF TABLES

Table	Page
3.1 Design Mix Proportions of Concrete	19
3.2 Test Results of Cubes after 28 days	19
3.3 Tensile Strength of reinforcing steel bars	22
3.4 Result of the Specimens	27
3.5 Relation between the torsional moment and angle of twist for (T2C).....	39
3.6 Relation between the torsional moment and angle of twist for (T3C).....	40
3.7 Relation between angle of twist and Torsional moment (Control Beam).....	42
3.8 Relation between angle of twist and Torsional moment (T3SU).....	43
3.9 Relation between angle of twist and Torsional moment (T3SUA).....	45
3.10 Relation between angle of twist and Torsional moment (T3SF).....	46
3.11 Relation between angle of twist and Torsional moment (T3S45).....	48
3.12 Relation between angle of twist and Torsional moment (T4SU).....	50
3.13 Relation between angle of twist and Torsional moment (T4SUA).....	52
3.14 Relation between angle of twist and Torsional moment (T4SF).....	54
3.15 Relation between angle of twist and Torsional moment (T4S45).....	56
3.16 Beam test parameters and material properties.....	57
4.1 Relation between angle of twist and Torsional moment (Control Beam).....	63
5.1 Study on contribution of FRP fabrics on torsional capacity.....	88

NOTATIONS

A_{st}	Area of steel
a	shear span
b_f	width of the flange
b_w	width of the web
d_f	depth of the flange
d_w	depth of the web
d	effective depth
d'	effective cover
D	Overall depth of the beam
ρ	reinforcing ratio
ρ_{max}	maximum reinforcing ratio
ϕ	diameter of the reinforcement
f_y	yield stress of the reinforcement bar
L	span length of the beam
P_u	ultimate load
λ	load enhancement ratio

ACRONYMS AND ABBREVIATIONS

ACI	American Concrete Institute
CB	Control Beam
CFRP	Carbon Fiber Reinforced Polymer
EB	Externally Bonded
FRP	Fiber Reinforced Polymer
FGPB	Fiber Glass Plate Bonding
GFRP	Glass Fiber Reinforced Polymer
HYSD	High-Yield Strength Deformed
IS	Indian Standard
NSM	Near Surface Mounted
PSC	Portland Slag Cement
RC	Reinforced Concrete
SB	Strengthened Beam

CHAPTER – 1

INTRODUCTION

CHAPTER 1

INTRODUCTION

1.1. OVERVIEW

Modern civilization relies upon the continuing performance of its civil engineering infrastructure ranging from industrial buildings to power stations and bridges. For the satisfactory performance of the existing structural system, the need for maintenance and strengthening is inevitable. During its whole life span, nearly all engineering structures ranging from residential buildings, an industrial building to power stations and bridges faces degradation or deteriorations. The main causes for those deteriorations are environmental effects including corrosion of steel, gradual loss of strength with ageing, variation in temperature, freeze-thaw cycles, repeated high intensity loading, contact with chemicals and saline water and exposure to ultra-violet radiations. Addition to these environmental effects earthquakes is also a major cause of deterioration of any structure. This problem needs development of successful structural retrofit technologies. So it is very important to have a check upon the continuing performance of the civil engineering infrastructures. The structural retrofit problem has two options, repair/retrofit or demolition/reconstruction. Demolition or reconstruction means complete replacement of an existing structure may not be a cost-effective solution and it is likely to become an increasing financial burden if upgrading is a viable alternative. Therefore, repair and rehabilitation of bridges, buildings, and other civil engineering structures is very often chosen over reconstruction for the damage caused due to degradation, aging, lack of maintenance, and severe earthquakes and changes in the current design requirements. Previously, the retrofitting of reinforced concrete structures, such as columns, beams another structural elements, was done by removing and replacing the low quality or damaged concrete or/and steel reinforcements with

new and stronger material. However, with the introduction of new advanced composite materials such as fiber reinforced polymer (FRP) composites, concrete members can now be easily and effectively strengthened using externally bonded FRP composites. Retrofitting of concrete structures with wrapping FRP sheets provide a more economical and technically superior alternative to the traditional techniques in many situations because it offers high strength, low weight, corrosion resistance, high fatigue resistance, easy and rapid installation and minimal change in structural geometry. In addition, FRP manufacturing offers a unique opportunity for the development of shapes and forms that would be difficult or impossible with the conventional steel materials. Although the fibers and resins used in FRP systems are relatively expensive compared with traditional strengthening materials, labour and equipment costs to install FRP systems are often lower. FRP systems can also be used in areas with limited access where traditional techniques would be impractical. Several investigators took up concrete beams and columns retrofitted with carbon fiber reinforced polymer (CFRP) glass fiber reinforced polymer (GFRP) composites in order to study the enhancement of strength and ductility, durability, effect of confinement, preparation of design guidelines and experimental investigations of these members. The results obtained from different investigations regarding enhancement in basic parameters like strength/stiffness, ductility and durability of structural members retrofitted with externally bonded FRP composites, though quite encouraging, still suffers from many limitations. This needs further study in order to arrive at recognizing FRP composites as a potential full proof structural additive. FRP repair is a simple way to increase both the strength and design life of a structure. Because of its high strength to weight ratio and resistance to corrosion, this repair method is ideal for deteriorated concrete structure.

1.2. TORSIONAL STRENGTHENING OF BEAMS

Early efforts for understanding the response of plain concrete subjected to pure torsion revealed that the material fails in tension rather than shear. Structural members curved in plan, members of a space frame, eccentrically loaded beams, curved box girders in bridges, spandrel beams in buildings, and spiral stair-cases are typical examples of the structural elements subjected to torsional moments and torsion cannot be neglected while designing such members. Structural members subjected to torsion are of different shapes such as T-shape, inverted L-shape, double T-shapes and box sections. These different configurations make the understanding of torsion in RC members of complex task. In addition, torsion is usually associated with bending moments and shearing forces, and the interaction among these forces is important. Thus, the behaviour of concrete elements in torsion is primarily governed by the tensile response of the material, particularly its tensile cracking characteristics. Spandrel beams, located at the perimeter of buildings, carry loads from slabs, joists, and beams from one side of the member only. This loading mechanism generates torsional forces that are transferred from the spandrel beams to the columns. Reinforced concrete (RC) beams have been found to be deficient in torsional capacity and in need of strengthening. These deficiencies occur for several reasons, such as insufficient stirrups resulting from construction errors or inadequate design, reduction in the effective steel area due to corrosion, or increased demand due to a change in occupancy. Similar to the flexure and shear strengthening, the FRP fabric is bonded to the tension surface of the RC members for torsion strengthening. In the case of torsion, all sides of the member are subjected to diagonal tension and therefore the FRP sheets should be applied to all the faces of the member cross section. However, it is not always possible to provide external reinforcement for all the surfaces of the member cross section. In cases of inaccessible sides of the cross section, additional means

of strengthening has to be provided to establish the adequate mechanism required to resist the torsion. The effectiveness of various wrapping configurations indicated that the fully wrapped beams performed better than using FRP in strips.

1.3. ADVANTAGES AND DISADVANTAGES OF FRP

1.3.1. Advantages

There have been several important advances in materials and techniques for structural rehabilitation, including a new class of structural materials such as fiber-reinforced polymers (FRP). One such technique for strengthening involves adding external reinforcement in the form of sheets made of FRP. Advanced materials offer the designer a new combination of properties not available from other materials and effective rehabilitation systems. Strengthening structural elements using FRP enables the designer to selectively increase their ductility, flexure, and shear capacity in response to the increasing seismic and service load demands. For columns, wrapping with FRP can significantly improve the strength and ductility.

A potent advantage of using FRP as an alternate external confinement to steel is the high strength to weight ratio comparisons. In order to achieve an equivalent confinement, FRP plates are up to 20% less dense than steel plates and are at least twice as strong, if not more. Manufacture of modern composites is, then, possible in reduced sections and allows composite plates to be shaped on-site. The lower density allows easier placement of confinement in application. Design of external confinement to a structure should be made with conservative adjustments to the primary structures dead weight load. Changes of the stiffness of members should be considered when redesigning the structure. The improved behaviour of FRP wrapped members reduces the strains of internal steel reinforcement thereby delaying attainment of yielding. Much like internal

steel confinement in longitudinal and lateral axes, external confinement exerts a similar pressure on the concrete as well as to the internal steel. Furthermore, FRP have high corrosive resistance equating to material longevity whilst within aggressive environments. Such durability makes for potential savings in long-term maintenance costs.

1.3.2. Disadvantages

With the above advantages FRP does also have some disadvantages as follows: The main disadvantage of externally strengthening structures with fiber composite materials is the risk of fire, vandalism or accidental damage, unless the strengthening is protected. As FRP materials are lightweight they tend to poses aerodynamic instability. Retrofitting using fiber composites are more costly than traditional techniques. Experience of the long-term durability of fiber composites is not yet available. This may be a disadvantage for structures for which a very long design life is required but can be overcome by appropriate monitoring. This technique need highly trained specialists. More over there is lack of standards and design guides.

1.4 ORGANIZATION OF THESIS

Chapter 1 gives a brief introduction to the use of GFRP as externally bonded reinforcement to strengthen the concrete members of buildings. This chapter also includes the advantages and disadvantages of FRP.

Chapter 2 reviews the literatures on prediction of torsional behaviour of RC beams wrapped with FRP have been discussed. The objectives and scope of the proposed research work are identified in this Chapter.

Chapter 3 discusses the details of experimental studies conducted and gives the test results of the beams which were tested under two-point loading arrangement.

Chapter 4 gives all the experimental results of all beams with different types of layering and orientation of GFRP. This chapter describes the failure modes, load-angle of twist analysis and ultimate load carrying capacity of the beams.

Finally, in Chapter 5, the summary and conclusions are given. Recommendations for improved methods for estimating torsional behaviour of longitudinal hole in the T beams and L beams are summarised. The scope for future work is also discussed.

CHAPTER – 2

REVIEW OF LITERATURE

CHAPTER 2

REVIEW OF LITERATURE

2.1.BRIEF REVIEW

Externally bonded, FRP sheets are currently being studied and applied around the world for the repair and strengthening of structural concrete members. Strengthening with Fiber Reinforced Polymers (FRP) composite materials in the form of external reinforcement is of great interest to the civil engineering community. FRP composite materials are of great interest to the civil engineering community because of their superior properties such as high stiffness and strength as well as ease of installation when compared to other repair materials. Also, the non-corrosive and nonmagnetic nature of the materials along with its resistance to chemicals made FRP an excellent option for external reinforcement.

Research on FRP material for use in concrete structures began in Europe in the mid 1950's by Rubinsky and Rubinsky, 1954 and Wines, J. C. et al., 1966. The pioneering work of bonded FRP system can be credited to Meier (Meier 1987); this work led to the first on-site repair by bonded FRP in Switzerland (Meier and Kaiser 1991). Japan developed its first FRP applications for repair of concrete chimneys in the early 1980s (ACI 440 1996). By 1997 more than 1500 concrete structures worldwide had been strengthened with externally bonded FRP materials. Thereafter, many FRP materials with different types of fibres have been developed. FRP products can take the form of bars, cables, 2-D and 3-D grids, sheet materials and laminates. With the increasing usage of new materials of FRP composites, many research works, on FRPs improvements of processing technology and other different aspects haven been performed.

Though several researchers have been engaged in the investigation of the strengthened concrete structures with externally bonded FRP sheets/laminates/fabrics, no country yet has national design code on design guidelines for the concrete structures retrofitted using FRP composites. However, several national guidelines (The Concrete Society, UK: 2004; ACI 440:2002; FIB: 2001; ISIS Canada: 2001; JBDPA: 1999) offer the state of the art in selection of FRP systems and design and detailing of structures incorporating FRP reinforcement. On the contrary, there exists a divergence of opinion about certain aspects of the design and detailing guidelines. This is to be expected as the use of the relatively new material develops worldwide. Much research is being carried out at institutions around the world and it is expected that design criteria will continue to be enhanced as the results of this research become known in the coming years.

Several investigators like Saadatmanesh et al., (1994); Shahawy, (2000) took up FRP strengthened circular or rectangular columns studying enhancement of strength and ductility, durability, effect of confinement, preparation of design guidelines and experimental investigations of these columns.

Saadatmanesh et al. (1994) studied the strength and ductility of concrete columns externally reinforced with fibre composite strap. Chaallal and Shahawy (2000) reported the experimental investigation of fiber reinforced polymer-wrapped reinforced concrete column under combined axial-flexural loading. Obaidat et al (2010) studied the Retrofitting of reinforced concrete beams using composite laminates and the main variables considered are the internal reinforcement ratio, position of retrofitting and the length of CFRP.

2.2 LITERATURE REVIEW ON TORSIONAL STRENGTHENING OF RC BEAM

Most of the research projects investigating the use of FRP focused on enhancing the flexural and shear behaviour, ductility, and confinement of concrete structural members. A limited number of mostly experimental studies were conducted to investigate torsion strengthening of RC members.

Ghobarah et al. (2002) conducted an experimental investigation on the improvement of the torsional resistance of reinforced concrete beams using fiber-reinforced polymer (FRP) fabric. A total of 11 beams were tested. Three beams were designated as control specimens and eight beams were strengthened by FRP wrapping of different configuration and then tested. Both glass and carbon fibers were used in the torsional resistance upgrade. Different wrapping designs were evaluated. The reinforced concrete beams were subjected to pure torsional moments. The load, twist angle of the beam, and strains were recorded. Improving the torsional resistance of reinforced concrete beams using FRP was demonstrated to be viable. The effectiveness of various wrapping configurations indicated that the fully wrapped beams performed better than using strips. The 45° orientation of the fibers ensures that the material is efficiently utilized

Panchacharam and Belarbi (2002) experimentally found out that externally bonded GFRP sheets can significantly increase both the cracking and the ultimate torsional capacity. The behaviour and performance of reinforced concrete member strengthened with externally bonded Glass FRP (GFRP) sheets subjected to pure torsion was presented. The variables considered in the experimental study include the fiber orientation, the number of beam faces strengthened (three or four), the effect of number of FRP plies used, and the influence of anchors in U-wrapped test beams. Experimental results reveal that externally bonded GFRP sheets can significantly increase both the cracking and the ultimate torsional capacity. Predicted strengths of the test

beams using the proposed theoretical models were found to be in good agreement with the experimental results.

Salom et al. (2004) conducted both experimental and analytical programs focused on the torsional strengthening of reinforced concrete spandrel beams using composite laminates. The variables considered in this study included fiber orientation, composite laminate, and effects of a laminate anchoring system. Current torsional strengthening and repair methods are time and resource intensive, and quite often very intrusive. The proposed method however, uses composite laminates to increase the torsional capacity of concrete beams.

Jing et al. (2005) made an experimental investigation on the response of reinforced concrete box beam under combined actions of bending moment, shear and cyclic torque, strengthened with externally bonded carbon fiber reinforced polymer sheets. Three strengthened box beams and one reference box beam were tested. The main parameters of this experiment were the amount of CFS and the wrapping schemes. The failure shapes, torsional capacities, deformation capacities, rigidity attenuations and hysteresis behaviours of specimens were studied in detail. The experimental results indicated that the contribution of externally bonded CFS to the aseismic capacity of box beam is significant. Based on the test results and analysis, restoring force model of CFS strengthened R.C. box beam under combined actions of bending moment, shear and cyclic torque was established.

Al-Mahaidi and Hii (2006) focuses on the bond-behaviour of externally bonded CFRP in an overall investigation of torsional strengthening of solid and box-section reinforced concrete beams. Significant levels of debonding prior to failure by CFRP rupture were measured in experiments with photogrammetry. Numerical work was carried out using non-linear finite

element (FE) modelling. Good agreement in terms of torque-twist behaviour, steel and CFRP reinforcement responses, and crack patterns was achieved. The addition of a bond-slip model between the CFRP reinforcement and concrete meant that the debonding mechanisms prior to and unique failure modes of all the specimens were modelled correctly as well. Numerical work was carried out using non-linear finite element (FE) modelling. Good agreement in terms of torque-twist behaviour, steel and CFRP reinforcement responses, and crack patterns was achieved.

Very few analytical models are available for predicting the section capacity (Ameliand Ronagh 2007; Hii and Al-Mahadi 2006; Rahal and Collins 1995). Santhakumar et al. (2007) presented the numerical study on unretrofitted and retrofitted reinforced concrete beams subjected to combined bending and torsion. Different ratios between twisting moment and bending moment are considered. The finite elements adopted by ANSYS are used for this study. For the purpose of validation of the finite element model developed, the numerical study is first carried out on the un-retrofitted reinforced concrete beams that were experimentally tested and reported in the literature. Then the study has been extended for the same reinforced concrete beams retrofitted with carbon fiber reinforced plastic composites with $\pm 45^\circ$ and $0/90^\circ$ fiber orientations. The present study reveals that the CFRP composites with $\pm 45^\circ$ fiber orientations are more effective in retrofitting the RC beams subjected to combined bending and torsion for higher torque to moment ratios.

Ameli et al. (2007) experimentally investigated together with a numerical study on reinforced concrete beams subjected to torsion that are strengthened with FRP wraps in a variety of configurations. Experimental results show that FRP wraps can increase the ultimate torque of fully wrapped beams considerably in addition to enhancing the ductility.

Chalioris (2007) addressed an analytical method for the prediction of the entire torsional behaviour of reinforced concrete (RC) beams strengthened with externally bonded fibre-reinforced-polymers (FRP) materials. The proposed approach combines two different theoretical models; a smeared crack analysis for plain concrete in torsion for the prediction of the elastic behaviour and the cracking torsional moment, and a properly modified softened truss theory for the description of the post-cracking torsional response and the calculation of the ultimate torque capacity. The contribution of the FRPs is implemented by specially developed (a) equations in a well-known truss model and (b) stress - strain relationships of softened and FRP-confined concrete. In order to check the accuracy of the proposed methodology an experimental program of 12 rectangular beams under torsion was conducted. Tested beams were retrofitted using epoxy-bonded Carbon FRP continuous sheets and discrete strips as external reinforcement. Strengthened beams with continuous sheets performed improved torsional behaviour and higher capacity than the beams with strips, since failure occurred due to fibre rupture. Comparisons between analytically predicted results and experimental ones indicated that the proposed behavioural model provides rational torque curves and calculates the torsional moments at cracking and at ultimate with satisfactory accuracy.

Hiiand Al-Mahaidi (2007) briefly recounted the experimental work in an overall investigation of torsional strengthening of solid and box-section reinforced concrete beams with externally bonded carbon fiber-reinforced polymer (CFRP).

Mohammadizadeh et al. (2008) found that the increase in CFRP contribution to torsional strength concerning the beams strengthened by one ply and two plies of CFRP sheets is close for various steel reinforcement ratios, when compared to increasing the total amount of steel reinforcement.

Behera et al. (2008) conducted an experimental programme consisting of casting and testing of beams with “U” wrap was conducted in the laboratory to study the effect of aspect ratio (ratio of depth to breadth), constituent materials of ferrocement (viz., number of mesh layers, yield strength of mesh layers and compressive strength of mortar) and concrete strength on ultimate torsional strength and twist. This experimental results briefly recounts that wrapping on three sides enhance the ultimate torque and twist.

Deifalla and Ghobarah (2010) developed an analytical model for the case of the RC beams strengthened in torsion. The model is based on the basics of the modified compression field theory, the hollow tube analogy, and the compatibility at the corner of the cross section. Several modifications were implemented to be able to take into account the effect of various parameters including various strengthening schemes where the FRP is not bonded to all beam faces, FRP contribution, and different failure modes. The model showed good agreement with the experimental results. The model predicted the strength more accurately than a previous model. The model predicted the FRP strain and the failure mode.

Mahmood and Mahmood (2011) conducted several experiments to study the torsional behaviour of prestressed concrete beams strengthened with CFRP sheets. They have taken eight medium-scale reinforced concrete beams (150mmx250mm) cross section and 2500mm long were constructed pure torsion test. All beams have four strands have no eccentricity (concentric) at neutral axis of section. There are classified into two group according uses of ordinary reinforcements. Where four beams with steel reinforcements, for representing partial prestressing beams, while other four beams have not steel reinforcements for representing full prestressing beams. The applied CFRP configurations are full wrap, U jacked, and stirrups with spacing equal to half the depth of beam along its entire length. The test results have shown that the

performance of fully wrapped prestressed beams is superior to those with other form of sheet wrapping. All the strengthened beams have shown a significant increase in the torsional strength compared with the reference beams. Also, this study included the nonlinear finite element analysis of the tested beams to predict a model for analyzing prestressed beams strengthening with CFRP sheets.

Zojaji and Kabir (2011) developed a new computational procedure to predict the full torsional response of reinforced concrete beams strengthened with Fiber Reinforced Plastics (FRPs), based on the Softened Membrane Model for Torsion (SMMT). To validate the proposed analytical model, torque-twist curves obtained from the theoretical approaches are compared with experimental ones for both solid and hollow rectangular sections.

Ban S. Abduljalil (2012). Strengthening of T beams in torsion by using carbon fiber reinforced polymer (CFRP). The experimental work includes investigation of five reinforced concrete T beams tested under pure torsion. Variables considered in the test program include; effect of flange strengthening, effect of fiber orientation (90° or 45° CFRP strips with respect to the beam longitudinal axis), and the effect of using additional longitudinal CFRP strips with transverse CFRP strips. Test results were discussed based on torque - twist behavior, beam elongations, CFRP strain, and influence of CFRP on cracking torque, ultimate torque and failure modes. Results indicate significant increases in ultimate torque capacity with the use of CFRP.

2.3 CRITICAL OBSERVATION FROM THE LITERATURE

From the above literature review it is clear that, none of these models predicted the full behaviour of RC beams wrapped with FRP, account for the fact that the FRP is not bonded to all

beam faces, predicted the failure mode, or predicted the effective FRP strain using equations developed based on testing FRP strengthened beams in torsion. The reason is the complexity of the torsion problem and the lack of adequate experimental results required to understand the full behaviour.

2.4 OBJECTIVE AND SCOPE OF THE PRESENT WORK

The objective of present study is to evaluate the effectiveness of the use of epoxy-bonded GFRP fabrics as external transverse reinforced to reinforced concrete beams with flanged cross sections (T-beam) subjected to torsion. Torsional results from eight strengthened beams are compared with the experimental result of 3 control beams without FRP applications. The following FRP configurations are examined

1. Completely wrapped T-beams with discrete FRP strip around the cross section making 90^0 with longitudinal axis of beam.
2. Completely wrapped T-beams with discrete FRP strip around the cross section making 45^0 with longitudinal axis of the beam.
3. U-jacketed T- beam with discrete FRP strip bonded on web of the beam and bottom sides of the flange.
4. U-jacketed T- beam with discrete FRP strip bonded on web to bottom sides of the flange and anchored with the FRP strips on top of the flange.

An RC T-beam is analyzed and designed for torsion like an RC rectangular beam, the effect of concrete on flange is neglected by codes. In the present study effect of flange part in resisting torsion is studied by changing flange width of controlled beams. Three beams with varying

flange widths designed to fail in torsion are cast and tested to complete failure. Their performances are compared with respect to a rectangular beam of same depth and web thickness.

And the results are validated numerical by using simplified model developed by A.Deifalla and A.Ghobarah ¹⁴.

CHAPTER - 3

EXPERIMENTAL PROGRAM

CHAPTER 3

EXPERIMENTAL STUDY

To study the most influential strengthening variables on torsional behavior a total of eleven medium scale reinforced concrete beams of 1900 mm long were constructed for this work. T-shaped beams, which are sorted in three groups (T2, T3 and T4) and were tested under combined bending torsion. Three numbers of beams are without torsional reinforcement were the control specimens and eight specimens were strengthened using epoxy-bonded glass FRP fabrics as external transverse reinforcement.

The cross-section of specimens was One beam were flanged beams with T-shaped with dimensions $b_w/D/b_f/d_f = 150/270/250/80$ mm (beams of series T2). In The series-B five beam specimens were flanged beams, and they dimensions are $b_w/D/b_f/d_f=150/270/350/80$ (beams of series T3). And also another five beam specimens were T-shaped cross-section and dimensions $b_w/D/b_f/d_f=150/270/350/80$ (beams of series T4). The cross-section of all beams shown in fig 3.1

Each group comprises one control specimen without transverse reinforcement. Specimens T2C were the control specimen of group-A, it had only longitudinal reinforcement; four deformed bars of diameter 20mm ϕ , and 10mm ϕ , at the corners of the cross-section, and control specimen of T3C, and T4C of series six longitudinal deformed bars of diameter 20 mm ϕ , 10mm ϕ , and 8mm ϕ , transverse bars of 8mm ϕ two legged stirrups. The other eight specimens of the experimental program included the same longitudinal reinforcement as the control specimens of their group and transverse reinforcement (steel stirrups).

Test beams were identified based on the following naming system. The first character in the name R (Rectangular), T (T-section) is used to identify the cross/section of beam. Second character is the dimensions of the beam. The third two characters are used to specify the strengthening in web or flange or both (U or UA). fourth character in the name (90, 45) is used to specify the fiber orientation with respect to the longitudinal axis of the beam.

3.1. CASTING OF SPECIMENS.

For conducting experiment, eleven reinforced concrete beam specimen of size as Shown in the fig (Length of main beam (L) = 1900mm, Breadth of main beam(b_w) = 150mm, Depth of main beam(D) = 270mm, Length of cantilever parts = 400mm, Width of cantilever part= 200mm, Depth of cantilever part= 270mm, Distance of cantilever part from end of the beam= 350mm) and all having the same reinforcement detailing are cast. The mix proportion is 0.5: 1:1.67:3.3 for water, cement, fine aggregate and course aggregate is taken. The mixing is done by using concrete mixture. The beams were cured for 28 days. For each beam three cubes, two cylinders and two prisms were casted to determine the compressive strength of concrete for 28 days.

3.2. MATERIAL PROPERTIES

3.2.1. Concrete

For conducting experiment, the proportions in the concrete mix are tabulated in Table 3.1 as per IS:456-2000. The water cement ratio is fixed at 0.55. The mixing is done by using concrete mixture. The beams are cured for 28 days. For each beam six 150x150x150 mm concrete cube specimens and six 150x300 mm cylinder specimens were made at the time of casting and were

kept for curing, to determine the compressive strength of concrete at the age of 7 days & 28 days are shown in table 3.2

Table 3.1 Design Mix Proportions of Concrete

Description	Cement	Sand (Fine Aggregate)	Coarse Aggregate	Water
Mix Proportion (by weight)	1	1.67	3.33	0.5

The compression tests on control and strengthened specimen of cubes are performed at 7 days and 28 days. The test results of cubes are presented in Table 3.2.

Table 3.2 Test Result of Cubes after 28 days

Specimen Name		Average Cube Compressive Strength (MPa)	Average Cylinder Compressive Strength (MPa)	Specimen Name		Average Cube Compressive Strength (MPa)	Average Cylinder Compressive Strength (MPa)
Group-A	T2C	29.23	25.62	Group-C	T4C	30.56	23.75
	T3C	30.05	20.12		T4SU	30.89	24.74
Group-B	T3SU	28.62	22.15		T4SUA	27.4	20.5
	T3SUA	29.12	23.56		T4SF	30.77	24.87

	T3SF	28.69	23.15		T4S45	29.83	21.68
	T3S45	28.12	22.12				

3.2.2. Cement

Cement is a material, generally in powdered form, which can be made into a paste usually by the addition of water and, when molded or poured, will set into a solid mass. Numerous organic compounds used for an adhering, or fastening materials, are called cements, but these are classified as adhesives, and the term cement alone means a construction material. The most widely used of the construction cements is Portland cement. It is bluish-gray powdered obtained by finely grinding the clinker made by strongly heating an intimate mixture of calcareous and argillaceous minerals. Portland Slag Cement (PSC) Konark Brand was used for this investigation. It is having a specific gravity of 2.96.

3.2.3. Fine Aggregate

Fine aggregate is an accumulation of grains of mineral matter derived from disintegration of rocks. It is distinguished from gravel only by the size of the grains or particles, but is distinct from clays which contain organic material. Sand is used for making mortar and concrete and for polishing and sandblasting. Sands containing a little clay are used for making molds in foundries. Clear sands are employed for filtering water. Here, the fine aggregate/sand is passing through 4.75 mm sieve and having a specific gravity of 2.64. The grading zone of fine aggregate is zone III as per Indian Standard specifications IS: 383-1970.

3.2.4. Coarse Aggregate

Coarse aggregates are the crushed stone is used for making concrete. The commercial stone is quarried, crushed, and graded. Much of the crushed stone used is granite, limestone, and trap rock. The coarse aggregates of two grades are used one retained on 10 mm size sieve and another grade contained aggregates retained on 20 mm size sieve. The maximum size of coarse aggregate was 20 mm and is having specific gravity of 2.88 grading confirming to IS: 383-1970.

3.2.5. Water

Water fit for drinking is generally considered good for making the concrete. Water should be free from acids, alkalis, oils, vegetables or other organic impurities. Soft water produces weaker concrete. Water has two functions in a concrete mix. Firstly, it reacts chemically with the cement to form a cement paste in which the inert aggregates are held in suspension until the cement paste has hardened. Secondly, it serves as a vehicle or lubricant in the mixture of fine aggregates and cement. Ordinary clean portable tap water is used for concrete mixing in all the mix.

3.2.6. Reinforcing Steel

High-Yield Strength Deformed (HYSD) bars confirming to IS 1786:1985. The longitudinal steel reinforcing bars were deformed, high-yield strength, with 20 ϕ mm 10 ϕ mm and 8mm ϕ diameter. The stirrups were made from deformed steel bars with 8 mm ϕ diameter.

Three coupons of steel bars were tested and yield strength of steel reinforcements used in this experimental program is determined under uni-axial tension accordance with ASTM specifications. The proof stress or yield strength of the specimens are averaged and shown in Table 3.3. The modulus of elasticity of steel bars was 2×10^5 MPa.

Table 3.3 Tensile Strength of reinforcing steel bars

Sl. no. of sample	Diameter of bar (mm)	0.2% Proof stress (N/mm ²)	Avg. Proof Stress (N/mm ²)
1	20	475	470
2	10	530	529
3	8	520	523

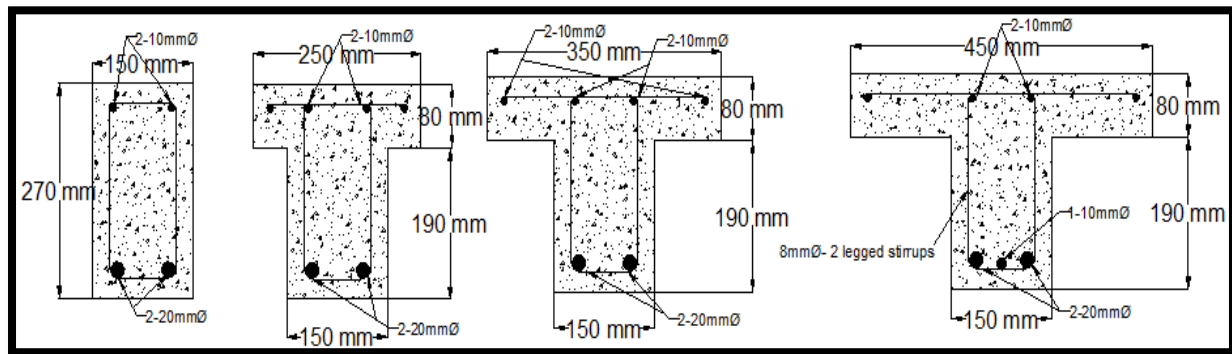


Figure 3-1. Detailing of Reinforcement

3.3. Mixing Of Concrete

Mixing of concrete is done thoroughly with the help of machine mixer so that a uniform quality of concrete was obtained.

3.3.1 Compaction

Compaction is done with the help of needle vibrator in all the specimens .And care is taken to avoid displacement of the reinforcement cage inside the form work. Then the surface of the concrete is levelled and smoothened by metal trowel and wooden float

3.3.2 Curing Of Concrete

Curing is done to prevent the loss of water which is essential for the process of hydration and hence for hardening. It also prevents the exposure of concrete to a hot atmosphere and to drying winds which may lead to quick drying out of moisture in the concrete and there by subject it to contraction stresses at a stage when the concrete would not be strong enough to resist them. Here curing is to be done by spraying water on the jute bags spread over the surface for a period of 7 days.

3.4 Fiber Reinforced Polymer (FRP)

Continuous fiber reinforced materials with polymeric matrix (FRP) can be considered as composite, heterogeneous, and anisotropic materials with a prevalent linear elastic behaviour up to failure. Normally, Glass and Carbon fibers are used as reinforcing material for FRP. Epoxy is used as the binding material between fiber layers.

For this study, GFRP sheet was used during the tests i.e., a bidirectional FRP with the fiber oriented in both longitudinal and transverse directions, due to the flexible nature and ease of handling and application, the FRP sheets are used for torsional strengthening. Throughout this study, E-glass was used manufactured by Owens Corning.

3.4.1 Epoxy Resin

The success of the strengthening technique primarily depends on the performance of the epoxy resin used for bonding of FRP to concrete surface. Numerous types of epoxy resins with a wide range of mechanical properties are commercially available in the market. These epoxy resins are generally available in two parts, a resin and a hardener. The resin and hardener used in this study are Araldite LY 556 and hardener HY 951 respectively.

3.4.2 Casting of GFRP Plate for tensile strength

There are two basic processes for moulding, that is, hand lay-up and spray-up. The hand lay-up process is the oldest, simplest, and most labour intense fabrication method. This process is the most common in FRP marine construction. In hand lay-up method liquid resin is placed along with reinforcement (woven glass fiber) against finished surface of an open mould. Chemical reactions in the resin harden the material to a strong, light weight product. The resin serves as the matrix for the reinforcing glass fibers, much as concrete acts as the matrix for steel reinforcing rods. The percentage of fiber and matrix was 50:50 by weight.

The following constituent materials are used for fabricating the GFRP plate:

- i. Glass FRP (GFRP)
- ii. Epoxy as resin
- iii. Hardener as diamine (catalyst)
- iv. Polyvinyl alcohol as a releasing agent

Contact moulding in an open mould by hand lay-up was used to combine plies of woven roving in the prescribed sequence. A flat plywood rigid platform was selected. A plastic sheet was kept on the plywood platform and a thin film of polyvinyl alcohol was applied as a releasing agent by use of spray gun. Laminating starts with the application of a gel coat (epoxy and hardener) deposited on the mould by brush, whose main purpose was to provide a smooth external surface and to protect the fibers from direct exposure to the environment. Ply was cut from roll of woven roving. Layers of reinforcement were placed on the mould at top of the gel coat and gel coat was applied again by brush. Any air bubble which may be entrapped was removed using serrated steel rollers. The process

of hand lay-up was the continuation of the above process before the gel coat had fully hardened. Again, a plastic sheet was covered the top of the plate by applying polyvinyl alcohol inside the sheet as releasing agent. Then, a heavy flat metal rigid platform was kept top of the plate for compressing purpose. The plates were left for a minimum of 48 hours before being transported and cut to exact shape for testing. Plates of 1 layer, 2 layers, 4 layers, 6 layers and 8 layers were casted and three specimens from each thickness were tested.



Figure 3-2. Specimens for tensile testing of woven Glass/Epoxy composite



Figure 3-3. Experimental setup of INSTRON universal testing Machine of 600 kN capacities



Figure 3-4. Specimen during testing

3.4.3 Determination of Ultimate Stress, Ultimate Load & Young's Modulus of FRP

The ultimate stress, ultimate load and young's modulus was determined experimentally by performing unidirectional tensile tests on specimens cut in longitudinal and transverse directions. The specimens were cut from the plates by diamond cutter or by hex saw. After cutting by hex

saw, it was polished with the help of polishing machine. At least three replicate sample specimens were tested and mean values adopted. The dimensions of the specimens are shown in below table 3.4.

For measuring the tensile strength and young's modulus, the specimen is loaded in INSTRON 600 kN in Production Engineering Lab, NIT, Rourkela. Specimens were gripped in the fixed upper jaw first and then gripped in the movable lower jaw. Gripping of the specimen should be proper to prevent the slippage. Here, it is taken as 50 mm from the each side. Initially, the strain is kept zero. The load, as well as the extension, was recorded digitally with the help of a load cell and an extensometer respectively. From these data, stress versus strain graph was plotted, the initial slope of which gives the young's modulus. The ultimate stress and ultimate load were obtained at the failure of the specimen. The average value of each layer of the specimens is given in the below Table 3.4.

Table 3.4 Result of the Specimens

GFRP plate of	Length of sample (mm)	Width of sample (mm)	Thickness of sample (mm)	Ultimate Load (N)	Young's Modulus (MPa)	Ultimate Stress (MPa)
1 layer	250	25	0.7	2760	5658	137.9
2 layers	250	25	1	4190	9493	167.7
4 layers	250	25	1.7	9400	10020	210.1

6 layers	250	25	2.1	13840	11000	276.8
8 layers	250	25	3.1	17720	9253	228.7

3.5 STRENGTHENING OF BEAMS

At the time of bonding of fiber, the concrete surface is made rough using a coarse sand paper texture and then cleaned with an air blower to remove all dirt and debris. After that the epoxy resin is mixed in accordance with manufacturer's instructions. The mixing is carried out in a plastic container (100 parts by weight of Araldite LY 556 to 10 parts by weight of Hardener HY 951). After their uniform mixing, the fabrics are cut according to the size then the epoxy resin is applied to the concrete surface. Then the GFRP sheet is placed on top of an epoxy resin coating and the resin is squeezed through the roving of the fabric with the roller. Air bubbles entrapped at the epoxy/concrete or an epoxy / fabric interface are eliminated. During hardening of the epoxy, a constant uniform pressure is applied to the composite fabric surface in order to extrude the excess epoxy resin and to ensure good contact between the epoxy, the concrete and the fabric. This operation is carried out at room temperature. Concrete beams strengthened with glass fiber



Fig. 3.5 Application of epoxy and hardener on the beam



Fig 3.6 Roller used for the removal of air bubble

3.6 Form Work

Fresh concrete being plastic in nature requires good form work to mold it to the required shape and size. So the form work should be rigid and strong to hold the weight of wet concrete without bulging anywhere. The joints of the form work are sealed to avoid leakage of cement slurry. Mobil oil was then applied to the inner faces of form work. The bottom rest over thick polythene sheet lead over the rigid floor. The reinforcement cage was then lowered, placed in position inside the side work carefully with a cover of 20mm on sides and bottom by placing concrete cover blocks.



Figure 3-7. Steel Frame Used For Casting of RC T-Beam

3.7. EXPERIMENTAL SETUP

The beams were tested in the loading frame of “Structural Engineering” Laboratory of National Institute of Technology, Rourkela. The testing procedure for the all the specimen is same. First the beams are cured for a period of 28 days then its surface is cleaned with the help of sand paper for clear visibility of cracks. The two-point loading arrangement was used for testing of beams.

This has the advantage of a substantial region of nearly uniform moment coupled with very small shears, enabling the bending capacity of the central portion to be assessed. Two-point loading is conveniently provided by the arrangement shown in Figure 3.9. The load is transmitted through a load cell and spherical seating on to a spreader beam. The spreader beam is installed on rollers seated on steel plates bedded on the test member with cement in order to provide a smooth levelled surface. The test member is supported on roller bearings acting on similar spreader plates. The specimen is placed over the two steel rollers bearing leaving 150 mm from the ends of the beam. The load is transmitted through a load cell via the square plates kept over the flange of the beam at a distance 100mm from the end. Loading was done by Hydraulic Jack of capacity 100 Tones. The below figure 3.8 shows the clear view of experimental setup

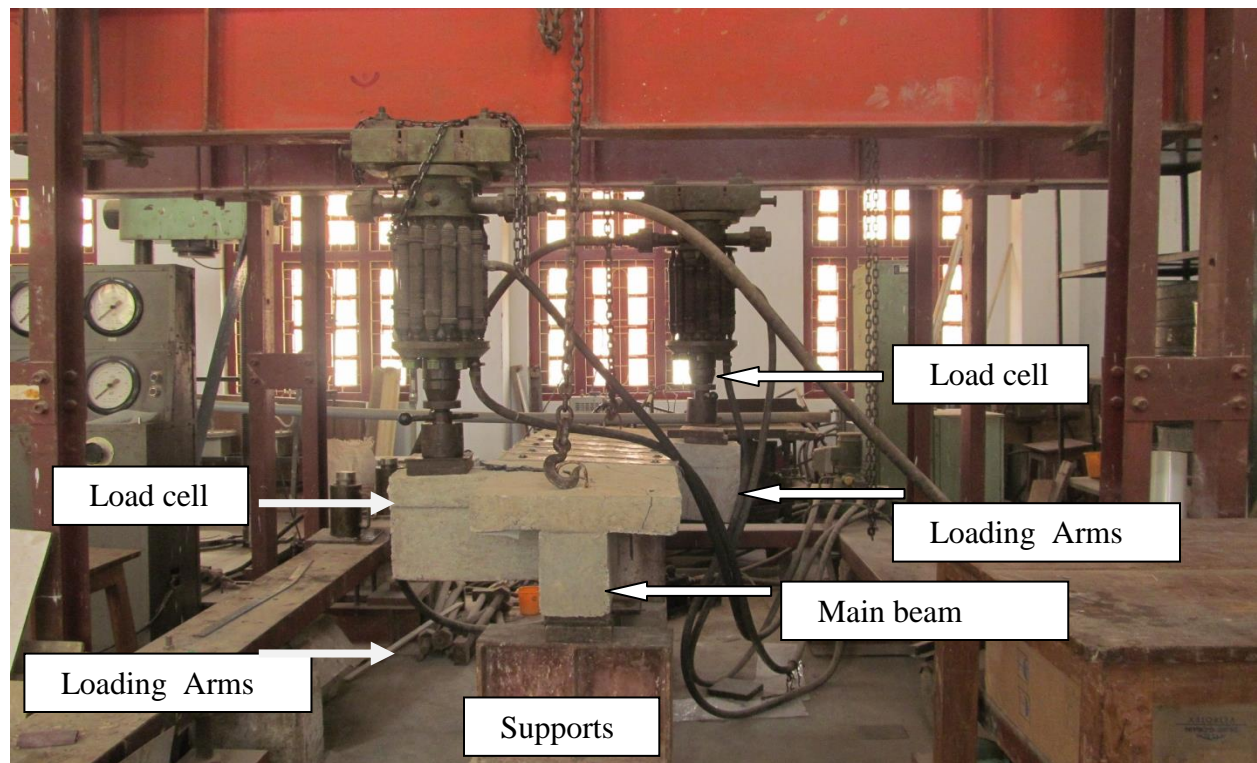


Fig no.3.8 Loading Setup

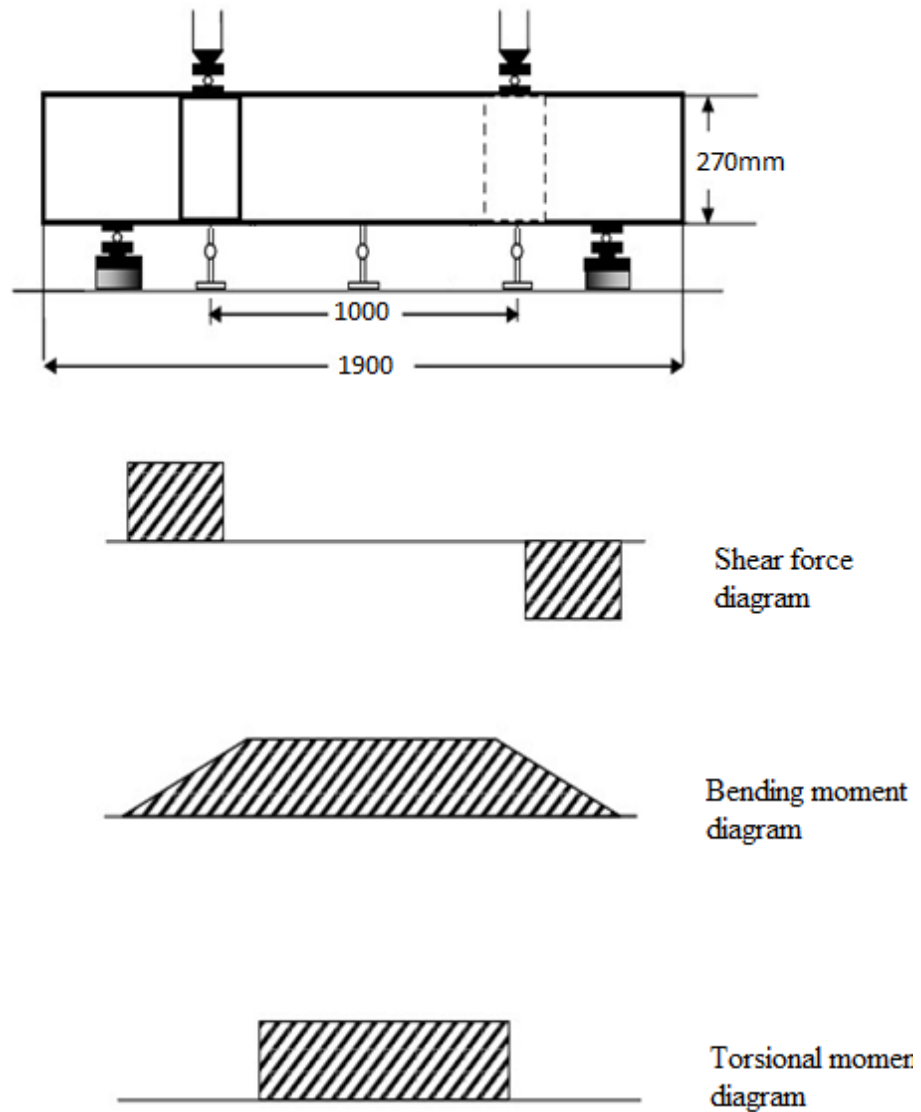


Fig. 3.9 Shear force and bending moment diagram for two point loading

3.8 DESCRIPTION OF SPECIMENS

The experimental program consists of 14 number of simply supported RC T-beams divided into four groups as mentioned earlier.

3.8.1 GROUP-A

3.8.1.1 T-Beam(T2C)

This group has one beam with 250 mm wide flanges and having reinforcement 2-20mm ϕ and 2-10mm ϕ as longitudinal reinforcement and without any torsional reinforcement to make the beams deficient in torsion. And this beam considered as control beam, there is no strengthening schemes are considered for this beam. shown in the fig. 3.9



Figure 3-10. Model of T-beam without GFRP and 250mm width of Flange, Control Beam

3.8.2 GROUP-B

In This group contains five numbers of beams with 350 mm flange width. And all the beams have same reinforcement i.e. 2-20mm ϕ , 2-10mm ϕ , and 2-8mm ϕ as longitudinal reinforcement and without any torsional reinforcement to make the beam deficient in torsion.

3.8.2.1 Control Beam (T3C)

For this control beam strengthening were not done. It is designed to know the behavior of the beam with flange in static loading test. And the fig.3.10 shows the control beam.



Figure 3-11.T-beam without GFRP and 350mm width of Flange, Control beam (T3C)

3.8.2.2 Strengthened T- beam (T3SU)

Third Beam is strengthened with fibre strips of 100 mm width at center to center spacing of 175 mm. The orientation of fibre strips are 90° with longitudinal axis of beam. Each strip has 4 layers of bi-directional woven GFRP and completely wrapped around the beam. And below fig 3.11 shows the beam.



Figure 3-12.T-beam Strengthened with GFRP of U-Wrap

3.8.2.3 Strengthened T- beam (T3SUA)

The beam (T3SUA) is modeled with four layers of GFRP strips having 100mm width and 75mm spacing of U-wrap on bottom and web portions and flange anchorage system provided, to control the debonding of FRP and figure 3-12.



Figure 3-13.T-beam Strengthened with GFRP of U-Wrap with flange anchorage.

3.8.2.4 Strengthened T- beam (T3SF)

The beam (T3SF) is modeled with four layers of GFRP strips having 100mm width and 75mm spacing of completely wrapped around the cross section of beam. And the orientation of beam has 90°. Figure 3-13.



Figure 3-14.T-beam Strengthened with GFRP of fully wrapped beam.

3.8.2.5 Strengthened T- beam (T3S45)

The beam (T3S45) is modeled with four layers of GFRP strips having 100mm width and 75mm spacing of fully wrapped on the beam and the strips having 45° inclination with the longitudinal section of the beam and figure shown in 3-14.



Figure 3-15.T-beam Strengthened with GFRP strips wrapped with an inclination of 45°

3.8.3 GROUP-C

In this group contains five numbers of beams including with the control beam. This beams has 450mm flange width and 2-20mm ϕ , 3-10mm ϕ , and 2-8mm ϕ of reinforcement for all the beams

3.8.3.1 T- BEAM (T4C)

The solid T- beam not strengthened with GFRP. It is designed to know the behavior of the beam with flange in static loading test. It is totally weak in Torsion mainly in center of the span. shown in the fig.3.15.



Figure 3-16.T-beam without GFRP and 450mm width of Flange, Control beam

In this group four beams were strengthened with GFRP and same strengthening schemes were considered for this group.fig 3.16-19



Figure 3-17.T-beam Strengthened with GFRP of U-Wrap



Figure 3-18.T-beam Strengthened with GFRP of U-Wrap with flange anchorage.

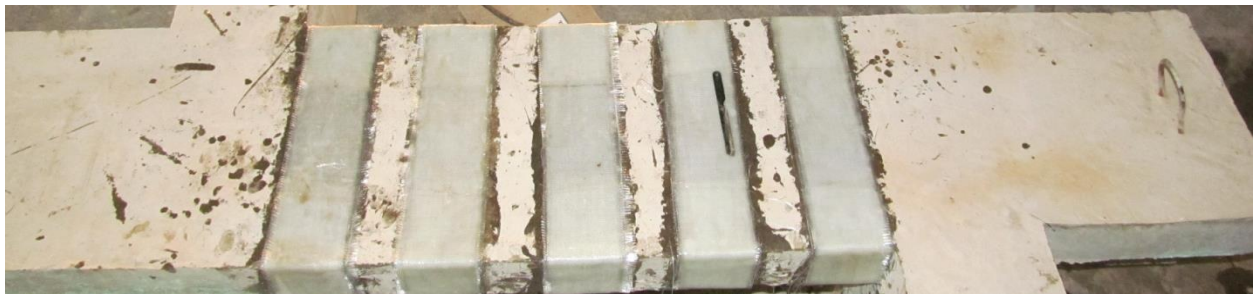


Figure 3-19.T-beam Strengthened with GFRP of fully wrapped beam.



Figure 3-20.T-beam Strengthened with GFRP strips wrapped with an inclination of 45°

3.9 TESTING OF BEAMS

All The eleven beams were tested one by one. Eight beams with FRP and three beams without FRP which is taken as the control Beams .All of them are tested in the above arrangement. The gradual increase in load and the deformation in the strain gauge reading are taken throughout the test. Load was applied on the two moment arm of the beams which is 0.375m away from the main beam.At each increment of the load, deflections at $L/3$, $L/2$ and $2L/3$ were observed and noted down with the help of six nos. of dial gauges. At each section two dial gauges were fixed to measure the displacement caused by twisting moment. The relative displacements divided by distance between dial gauges gives angle of twist. Section at $L/3$ was taken as sec-1, section at middle of beam as taken as sec-2, and section at $2L/3$ was taken as section 3.The loading arrangement was same for all the beams. The load at which the first visible crack is developed is recorded as cracking load. Then the load is applied till the ultimate failure of the beam. The deflections at two salient points mentioned for the beams with and without GFRP are recorded with respect to increase of load and angle of twist is been calculated and are furnished in table. The data furnished in this chapter have been interpreted and discussed in the next chapter to obtain a conclusion.

3.9.1 BEAM (T2C)



Fig.3.21 cracks pattern in beam

Table 3.5. Relation between the torsional moment and angle of twist for (T2C)

Twisting moment T in Kn-m	Angle of twist in section 2 (rad/m)	Angle of twist in section 3 (rad/m)	Remarks
0.00	0.000	0.000	
1.88	0.002	0.001	
3.75	0.003	0.004	
5.63	0.004	0.006	
7.50	0.006	0.008	
9.38	0.006	0.010	
11.25	0.008	0.013	
13.13	0.010	0.016	First Hair line Crack appeared @ 80kN
15.00	0.011	0.019	
16.88	0.014	0.024	Ultimate load @ 102 kN
18.75	0.017		

3.9.2 BEAM (T3C)



Fig.3.22 cracks pattern in beam

Table 3.6. Relation between the torsional moment and angle of twist for (T3C)

Twisting moment T in Kn-m	Angle of twist in section 1 (rad/m)	Angle of twist in section 2 (rad/m)	Remarks
0.00	0.000	0.000	
1.88	0.003	0.003	
5.63	0.006	0.006	
7.50	0.006	0.007	
11.25	0.008	0.009	
15.00	0.011	0.014	
16.88	0.012	0.018	First Hair line Crack appeared @90kN
20.63	0.013	0.022	
21.75			Ultimate load @ 116 kN

3.9.3 BEAM (T4C)



3.23a Control Beam after cracking (T4C)



3.23b Crack pattern at face-1



3.23c Crack pattern at face-2

Table 3.7 Relation between angle of twist and Torsional moment (Control Beam)

Twisting moment T in (Kn-m)	Angle of twist in section 1 (rad/m)	Angle of twist in section 2 (rad/m)	Remarks
0	0	0	
1.875	0.0022	0.0026	
3.75	0.0030	0.0037	
5.625	0.0037	0.0049	
7.5	0.0046	0.0059	
9.375	0.0059	0.0069	
11.25	0.0065	0.0082	
13.125	0.0071	0.0092	
15	0.0077	0.0107	
16.875	0.0082	0.0123	
18.75	0.0087	0.0139	
20.625	0.0095	0.0157	
22.5	0.0104	0.0181	First Hair line Crack appeared @120 kN
24.375	0.0127	0.0204	
26.25			
28.5			Ultimate load @ 152 kN

3.9.4 BEAM (T3SU)

Beam with U-wrapped GFRP in web portion (T3SU).



3.24a U- Wrapped beam after cracking



3.24b Closed view of cracks



3.24c Crack pattern in flange

Table 3.8 Relation between angle of twist and Torsional moment (T3SU)

Twisting moment T in Kn-m	Angle of twist in section 1 (rad/m)	Angle of twist in section 2 (rad/m)	Remarks
0	0	0	
1.875	0.004	0.003	
3.75	0.004	0.003	
5.625	0.005	0.004	
7.5	0.006	0.005	
9.375	0.007	0.006	
11.25	0.008	0.007	
13.125	0.010	0.008	
15	0.012	0.010	
16.875	0.014	0.011	
18.75	0.016	0.013	
20.625	0.018	0.014	First Hair line Crack appeared @ 110 kN
22.5	0.021	0.017	
24.375	0.024	0.019	
26.25	0.026	0.020	
26.8125			Ultimate load @ 143 kN

3.9.5 BEAM (T3SUA)

Beam with U-wrap with flange anchorage system of GFRP (T3SUA).



Fig. 3.25a Experimental Setup of the U-Wrap with Anchorage system Beam No.6 (T3SUA)



Fig 3.25b Closed view of Cracks



Fig 3.25c Cracks on Flange of Beam

Table 3.9 Relation between angle of twist and Torsional moment (T3SUA)

Twisting moment T in (Kn-m)	Angle of twist in section 1 (rad/m)	Angle of twist in section 2 (rad/m)	Remarks
0	0	0	
1.875	0.002	0.004	
3.75	0.003	0.006	
5.625	0.005	0.007	
7.5	0.006	0.008	
9.375	0.008	0.010	
11.25	0.010	0.012	
13.125	0.013	0.014	
15	0.015	0.017	
16.875	0.018	0.019	
18.75	0.022	0.021	First Hair line Crack appeared @ 100 kN
20.625	0.026	0.025	
22.5	0.032	0.027	
24.375	0.037	0.031	
26.25	0.043	0.032	
28.875			Ultimate load @ 154 kN

3.9.6 BEAM (T3SF)

Beam Fully wrapped with 100mm strips of GFRP (T3SF) 90°



Fig 3.26a Fully Wrapped beam after Cracking



Fig 3.26b Cracks on Flange of Beam



Fig 3.26c Closed view of Cracks

Table 3.10 Relation between angle of twist and Torsional moment (T3SF)

Twisting moment T in (Kn-m)	Angle of twist in section 1 (rad/m)	Angle of twist in section 2 (rad/m)	Remarks
0	0	0	
1.88	0.004	0.003	
3.75	0.005	0.003	
5.63	0.006	0.004	
7.50	0.006	0.005	
8.44	0.006	0.005	
9.38	0.007	0.005	
11.25	0.007	0.006	
13.13	0.007	0.006	
14.06	0.008	0.007	
15.00	0.008	0.007	
16.88	0.008	0.008	
18.75	0.009	0.008	
20.63	0.011	0.010	
22.50	0.012	0.011	
24.38	0.015	0.011	
26.25	0.017	0.012	

28.13	0.019	0.012	
30.00	0.021	0.013	
31.88	0.023	0.014	
33.75	0.025	0.015	
35.63	0.027	0.016	
37.50	0.030	0.017	
39.38	0.032	0.019	First Hair line Crack appeared @ 210 kN
41.25	0.037	0.020	
43.13			Ultimate load @ 230 kN

3.9.7 BEAM (T3S45)

Beam wrapped with 100mm Bi-directional GFRP (45°)



Fig 3.27a Beam wrapped with 100mm Bi-directional GFRP (45°) after cracking.



Fig.3.27b Closed view of cracks



Fig.3.27c crack in the flange

Table 3.11 Relation between angle of twist and Torsional moment (T3S45)

Twisting moment T in Kn-m	Angle of twist in section 1 (rad/m)	Angle of twist in section 2 (rad/m)	Remarks
0	0	0	
1.88	0.001	0.000	
3.75	0.001	0.001	
5.63	0.001	0.001	
7.50	0.002	0.003	
9.38	0.003	0.004	
11.25	0.004	0.005	
13.13	0.005	0.007	
15.00	0.006	0.008	
16.88	0.007	0.011	
18.75	0.008	0.013	
20.63	0.009	0.014	
22.50	0.011	0.018	
24.38	0.011	0.019	
26.25	0.012	0.022	
28.13	0.013	0.023	
30.00	0.014	0.026	

31.88	0.014	0.027	
33.75	0.015	0.030	
35.63	0.015	0.031	First Hair line Crack appeared @ 190 kN
37.5	0.023	0.033	
39.375			Ultimate load @ 210 kN

3.9.8 BEAM (T4SU)

Beam with U-wrapped GFRP in web portion (T4SU)



Fig.3.28a Beam 450mm flange strengthened with GFRP (U-Wrap)



Fig 3.28b Crack pattern at the main beam

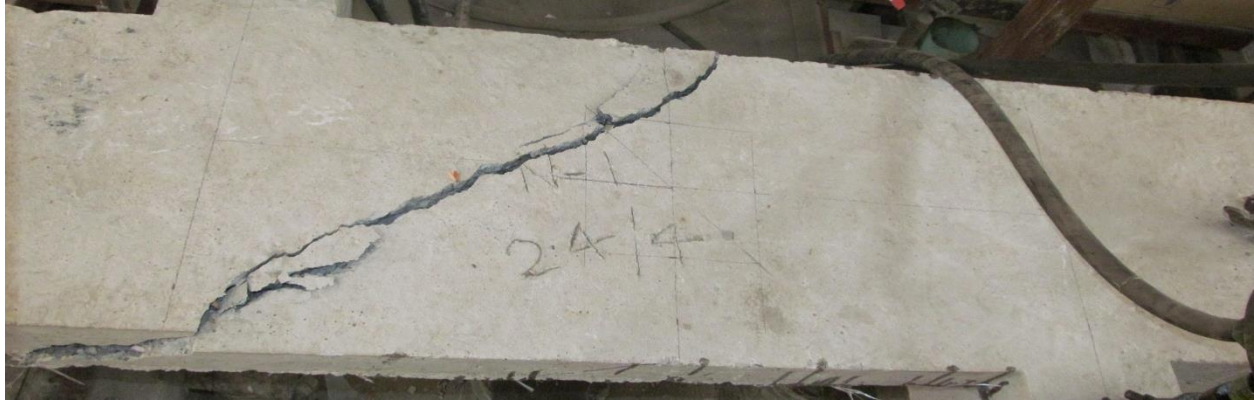


Fig 3.28c Cracks in the flange portion.

Table 3.12 Relation between angle of twist and Torsional moment (T4SU)

Twisting moment T in kN-m	Angle of twist in section 1 (rad/m)	Angle of twist in section 2 (rad/m)	Remarks
0	0	0	
1.88	0.000	0.000	
3.75	0.001	0.001	
5.63	0.002	0.003	
7.50	0.003	0.004	
9.38	0.003	0.004	
11.25	0.003	0.004	
13.13	0.004	0.005	
15.00	0.005	0.006	
16.88	0.005	0.007	
18.75	0.006	0.007	
20.63	0.008	0.011	
22.50	0.009	0.013	
24.38	0.010	0.013	
26.25	0.010	0.015	
28.13	0.012	0.015	
30.00	0.015	0.015	
31.88	0.018	0.016	First Hair line Crack appeared @160 kN
33.75	0.020	0.016	
35.63	0.027	0.019	

37.50	0.033	0.020	
39.00			Ultimate load @ 208 kN

3.9.9 BEAM (T4SUA)

Beam with U-wrap with flange anchorage system of GFRP (T4SUA)



Fig.3.29a Beam with U-wrap with flange anchorage system of GFRP (T4SUA)



Fig.3.29b closed view of crack



Fig.3.29c Crack in web portion

Table 3.13 Relation between angle of twist and Torsional moment (T4SUA)

Twisting moment T in Kn-m	Angle of twist in section 1 (rad/m)	Angle of twist in section 2 (rad/m)	Remarks
0	0	0	
1.88	0.002	0.000	
3.75	0.002	0.000	
5.63	0.003	0.001	
7.50	0.003	0.002	
9.38	0.004	0.002	
11.25	0.005	0.003	
13.13	0.006	0.004	
15.00	0.007	0.006	
16.88	0.007	0.006	
18.75	0.008	0.008	
20.63	0.009	0.008	
22.50	0.010	0.010	
24.38	0.010	0.011	
26.25	0.011	0.012	
28.13	0.012	0.014	
30.00	0.013	0.016	
31.88	0.013	0.018	
33.75	0.015	0.020	
35.63	0.016	0.021	
37.50	0.016	0.023	
39.38	0.017	0.025	First Hair line Crack appeared @210 kN
41.25	0.017	0.028	
43.13	0.016	0.029	
45.00	0.017	0.029	
46.13			Ultimate load @ 246 kN

3.9.10 BEAM (T4SF)

Beam with 450mm wide flange strengthened with full wrap (T4SF).



Fig 3.30a Fully Wrapped beam after Cracking of 450mm wide flange

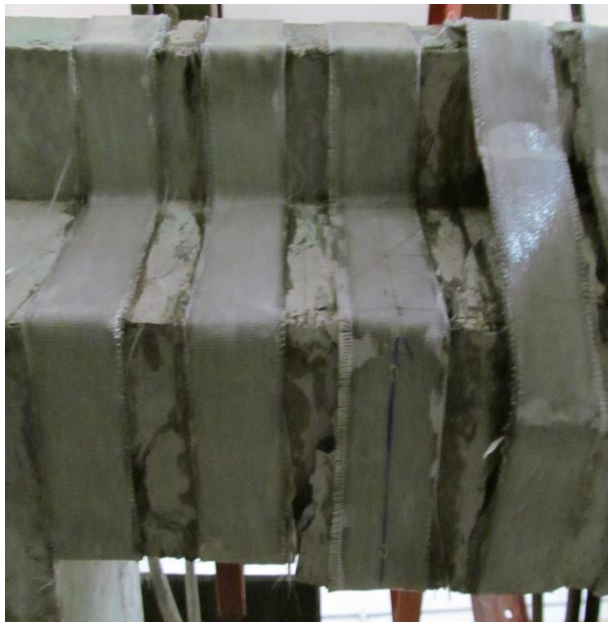


Fig.3.30b debonding of FRP in web



Fig.3.30c cracks in flange

Table 3.14 Relation between angle of twist and Torsional moment (T4SF)

Twisting moment T in Kn-m	Angle of twist in section 1 (rad/m)	Angle of twist in section 2 (rad/m)	Remarks
0	0	0	
1.88	0.004	0.003	
3.75	0.005	0.004	
5.63	0.006	0.005	
7.50	0.007	0.006	
9.38	0.008	0.008	
11.25	0.009	0.008	
13.13	0.010	0.008	
15.00	0.011	0.009	
16.88	0.014	0.013	
18.75	0.016	0.013	
20.63	0.016	0.015	
22.50	0.017	0.016	
24.38	0.019	0.018	
26.25	0.020	0.019	
28.13	0.022	0.020	
30.00	0.023	0.022	
31.88	0.028	0.027	
33.75	0.028	0.028	
35.63	0.030	0.028	
37.50	0.031	0.030	
39.38	0.033	0.032	
41.25	0.035	0.034	
43.13	0.037	0.037	
45.00	0.039	0.040	
46.88	0.037	0.040	
48.75	0.037	0.040	First Hair line Crack appeared @260 kN
50.63	0.038	0.041	
52.50	0.037	0.039	
54.38	0.035	0.039	
56.25			
58.13			Ultimate load @ 315 kN

3.9.11 BEAM (T4S45)

Beam wrapped with 100mm Bi-directional GFRP (45°)



Fig.3.31a cracks in the web portion for 45° wrapping

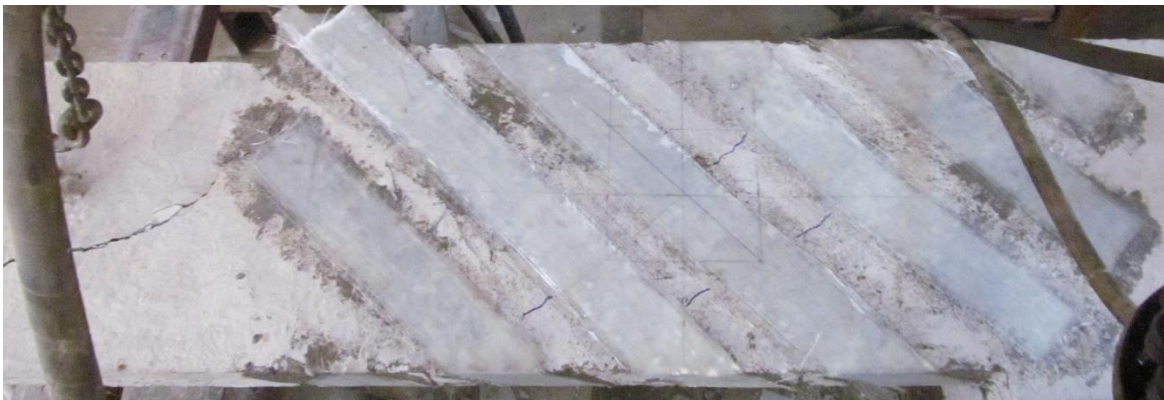


Fig3.31b Debonding of FRP near the loading arm



Fig.3.31c Rupture in the GFRP

Table 3.15 Relation between angle of twist and Torsional moment (T4S45)

Twisting moment T in Kn-m	Angle of twist in section 1 (rad/m)	Angle of twist in section 2 (rad/m)	Remarks
0	0	0	
1.88	0.004	0.003	
3.75	0.005	0.004	
5.63	0.006	0.005	
7.50	0.007	0.006	
9.38	0.008	0.008	
11.25	0.009	0.008	
13.13	0.009	0.008	
15.00	0.010	0.009	
16.88	0.014	0.013	
18.75	0.016	0.015	
20.63	0.016	0.015	
22.50	0.017	0.016	
24.38	0.019	0.018	
26.25	0.020	0.019	
28.13	0.022	0.020	
30.00	0.023	0.022	
31.88	0.028	0.027	
33.75	0.028	0.027	
35.63	0.029	0.028	
37.50	0.030	0.030	
39.38	0.032	0.032	
41.25	0.034	0.034	
43.13	0.036	0.037	First Hair line Crack appeared @230 kN
45.00	0.037	0.040	
46.88			
48.75			
50.63			
52.50			
54.38			
56.25			Ultimate load @ 297 kN

3.10 SUMMARY

Fourteen beams were tested in this experimental investigation. four control beams was tested, five beams were strengthened with different orientations of GFRP, two beams were strengthened with epoxy bonded GFRP with anchorage system to avoid debonding and other two beams were strengthened with providing stirrups in the flange portion . The detail descriptions of above mentioned beams are presented in Table 3.5.

Table 3.16 Beam test parameters and material properties

Beam ID		f_c (MPa)	Tension Reinforcement	Yield Stress, f_y (MPa)	Material Type	Sheet Thickness (mm)	Strengthening system with GFRP sheets
Group- A	T2C	20.93	2-20mm ϕ ,	470	--	--	Control Beam
	T3C	21.86	2-20mm ϕ ,	470		--	Control Beam
Group- B	T3SU	23.72	2-20mm ϕ ,	470	GFRP	1.7	four layers of strips,(100mm) continuous bonded to bottom and sides of beam (U-Wrap)
	T3SUA	20.46	2-20mm ϕ ,	470	GFRP	1.7	four layers of strips (100mm), continuous bonded to the bottom and sides of beam with flange anchorage system

	T3SF	26.82	2-20mm ϕ ,	470	GFRP	1.7	Four layers of strips continuous bonded with the full length of the beam
Group-C	T3S45		2-20mm ϕ ,	470		1.7	Four layers of strips (100mm), were layered with an inclination of 45° to the longitudinal section of beam
	T4C	22.75	2-20mm ϕ , 1-10mm ϕ	470 529	-	-	Control Beam
	T4SU	20.74	2-20mm ϕ , 1-10mm ϕ	470 529	GFRP	1.7	four layers of strips,(100mm) continuous bonded to bottom and sides of beam (U-Wrap)
	T4SUA	23.5	2-20mm ϕ , 1-10mm ϕ	470 529	GFRP	1.7	four layers of strips (100mm), continuous bonded to the bottom and sides of beam with flange anchorage system
	T4SF	24.87	2-20mm ϕ , 1-10mm ϕ	470 529	GFRP	1.7	Four layers of strips continuous bonded with the full length of the beam
	T3S45		2-20mm ϕ , 1-10mm ϕ ,	470 529	GFRP	1.7	Four layers of strips (100mm), were layered with an inclination of 45° to the longitudinal section of beam

CHAPTER-4

TEST RESULTS & DISCUSSIONS

CHAPTER 4

TEST RESULTS AND DISCUSSIONS

4.1 EXPERIMENTAL RESULTS

This chapter includes experimental results of all beams with different types of configurations and orientation of GFRP. Their behavior throughout the test is described using recorded data on torsional behavior and the ultimate load carrying capacity. The crack patterns and the mode of failure of each beam are also described in this chapter. All the beams are tested till complete failure. Beams T2C, T3C and T4C are the control beams. It is observed that the control beam had less load carrying capacity and high deflection values compared to that of the FRP strengthened beams. Group A beam T2C has 250 mm wide flange beam is considered as control beam. In group-B and group-C, all beams are strengthened with 100mm wide ,four layered strips of GFRP fabrics with an clear spacing of 75 mm. The different patterns of wrapping adopted are 90 degree fully wrapped, 45° fully wrapped, U-wrapped, U-wrap with flange anchored with bolt.

4.2 FAILURE MODES

Different failure modes have been observed in the experiments .These include torsional shear failure due to GFRP rupture and debonding .Rupture of the FRP strips is assumed to occur if the strain in the FRP reaches its design rupture strain before the concrete reaches its maximum usable strain. GFRP debonding can occur if the force in the FRP cannot be sustained by the substrate. Load was applied on the two moment arm of the beams which is 0.375m away from the main beam. At each increment of the load, deflections at $L/3$, $L/2$ and $2L/3$ were observed and noted down with the help of six nos. of dial gauges. At each section two dial gauges were

fixed to measure the displacement caused by twisting moment. The relative displacements divided by distance between dial gauges gives angle of twist. Section at $L/3$ was taken as sec-1, section at middle of beam as taken as sec-2, and section at $2L/3$ was taken as section 3. The loading arrangement was same for all the beams.

4.3 TORSIONAL MOMENT AND ANGLE OF TWIST ANALYSIS

4.3.1 Torsional moment and Angle of twist Analysis of all Beams

Here the angle of twist of each beam is analyzed. Angle of twist of each beam is compared with the angle of twist of control beam. Also the torsional behaviors compared between different wrapping schemes having the same reinforcement. Same type of load arrangement was done for all the beams. All the beams were strengthened by application of GFRP in four layers over the beams. It was noted that the behavior of the beams strengthen with GFRP sheets are better than the control beams. The deflections are lower when beam was wrapped externally with GFRP strips. The use of GFRP strips had effect in delaying the growth of crack formation.

When all the wrapping schemes are considered it was found that the Beam with GFRP strips fully wrapped and 45° orientation over full a length of 0.8m in the middle part had a better resistant to torsional behavior as compared to the others strengthened beams with GFRP

4.3.1.1 Control Beam (R1C)



Fig. 4.1a Experimental Setup of the Control Beam R1C



Fig.4.1b Crack pattern at face-1

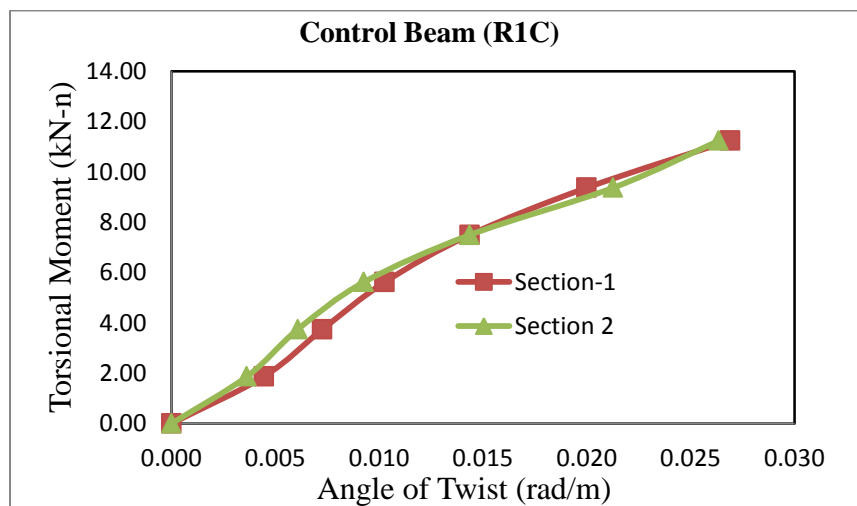


Fig.4.1c crack pattern face-2

Table 4.1 Relation between angle of twist and Torsional moment (Control Beam)

Twisting moment T in kN-m	Angle of twist in section 1 (rad/m)	Angle of twist in section 2 (rad/m)	Remarks
0.00	0.000	0.000	
1.88	0.001	0.004	
3.75	0.001	0.007	
5.63	0.002	0.010	
7.50	0.002	0.014	
9.38	0.004	0.020	
11.25	0.007	0.027	First Hair line Crack appeared @80kN
12.75			Ultimate load @ 90kN

Beam R1C rectangular beam is unstrengthen beam and considered as the control beam .This beam was not a part of this study but had been taken from previous study. The details of data are given in Table 4.1. This beam has same reinforcement detail and dimensions. This is included into the present study to compare the effect of concrete in flange on torsional behavior of RC beams.

**Fig 4.2 Torsional moment Vs Angle of Twist for Beam R1C**

4.3.1.2 BEAM (T2C)

Beam T2C is flanged RC beam with 250 mm wide flange. This beam was cast and tested to study effect of flange width on torsional behavior of T-Beam. In various design Codes a flange RC beam is designed like rectangular beam for torsion assuming that the shear flow takes place around the stirrups provided in the web portion only. The contribution of flange area in resisting torsional moment is neglected.



Fig. 4.3 Cracks Pattern in T2C

The first hair line inclined crack initiated at load of 80 kN and propagated spirally across the section along with various small inclined cracks. The beam failed at 102 kN load i.e. at 19.175 kNm torsional moment. It was observed those cracks were appeared making an angle 40° - 50° with the main beam. The cracks were developed in a spiral pattern all over the main beam which later leads to the collapse of the beam in torsional shear.

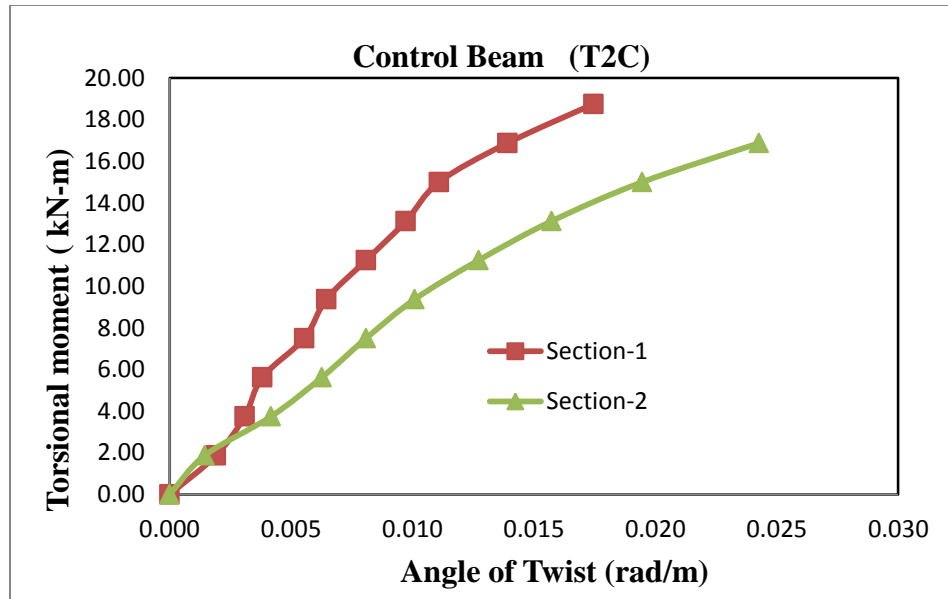


Fig 4.4 Torsional moment Vs Angle of Twist for Beam T2C

4.3.1.3. BEAM (T3C)

Beam T3C is RC T-beam with 350 mm wide flange. This beam was taken as control beam for series B. This beam is also considered to study the effect of flange area on torsional capacity of RC T-beam.



Fig. 4.5 Spiral crack in the beam

While testing initial hairline cracks appeared at 90 kN load. First crack appeared on the flange and with further increase of load propagated diagonally towards web on both sides. Beam failed completely in torsion at a load 116kN and torsional moment 21.75kNm. The cracks were appeared making an angle 45° with the axis of the main beam. The cracks were developed in a spiral pattern all over the main beam as shown in Fig.4.5 which later leads to the collapse of the beam in torsional shear. Diagonal cracks propagated in opposite direction and vertical faces, both sides and bottom.

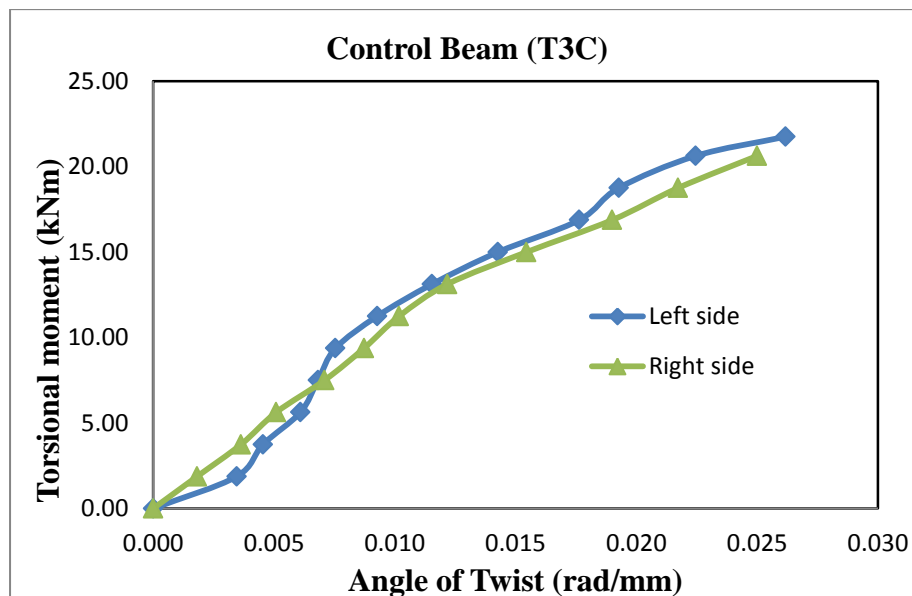


Fig 4.6 Torsional moment Vs Angle of Twist curve (T3C)

4.3.1.4 BEAM (T3SU)

The Beam T3SU was strengthened with four layers of bi-directional GFRP strips having U-wrap for web and bottom of the flange. The strips were 100 mm wide and applied @ 175 mm center to center. At the load of 110 kN initial hairline diagonal cracks appeared on flange as shown in the Fig.4.7b. With the increase of load diagonal cracks appeared in the concrete between the FRP

strips making approximately. This is because strips acted like external reinforcement .Further increasing the load FRP debonding takes place at the ultimate load 143 kN and torsional moment 26.81 kNm.T3SU resulted in a 23.27% increase in torsional capacity over the control beam. It was observed that cracks were appeared making an angle 55° - 65° with the axis of main beam.The debonding of FRP were occurred and cracks were developed in a spiral pattern all over the main beam which later leads to the collapse of the beam in torsional shear.



4.7(a) Initial hairline crack

4.7(b)Crack at ultimate load

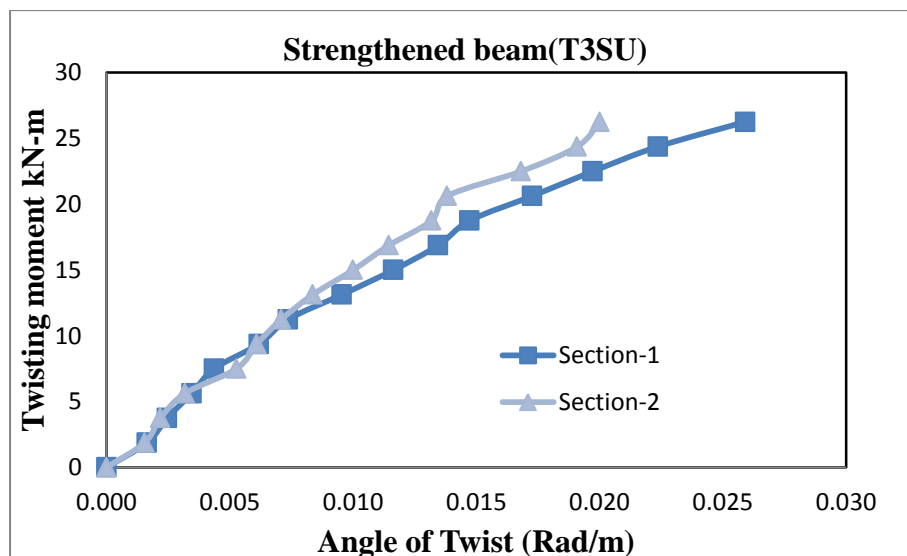


Fig 4.8 Torsional moment Vs Angle of Twist curve (T3SU)

4.3.1.5 BEAM (T3SUA)

The Beam T3SUA was strengthened with four layers of bi-directional GFRP strips of 100 mm width @ 175 mm c/c having U-wrap for web and bottom of the flange, and top of the flange. The FRP were not applied on vertical sides of the flange. This causes discontinuity to the shear flow along FRP. One anchor bolt is used on each sides of the flange and on each strip of FRP. Anchor threaded bolts carry axial tension force as a part of the shear flow resisting mechanism developed to resist the applied torsion.



Fig 4.9(a) Closed view of Cracks



Fig 4.9(b) Cracks on Flange of Beam

At the load of 100 kN initial hairline cracks appeared. Later with the increase in loading values the crack propagated further. It has failed completely in torsion at a load 154kN and torsional moment 28.875 KNm. The increase strength of beam was 32.75% as the control beam. It was observed those cracks were initially generated in the flange. The fig.4.9b shows rupture of FRP was occurred and cracks were developed in a spiral pattern all over the main beam. The cracks were generated making an angle of 42° .

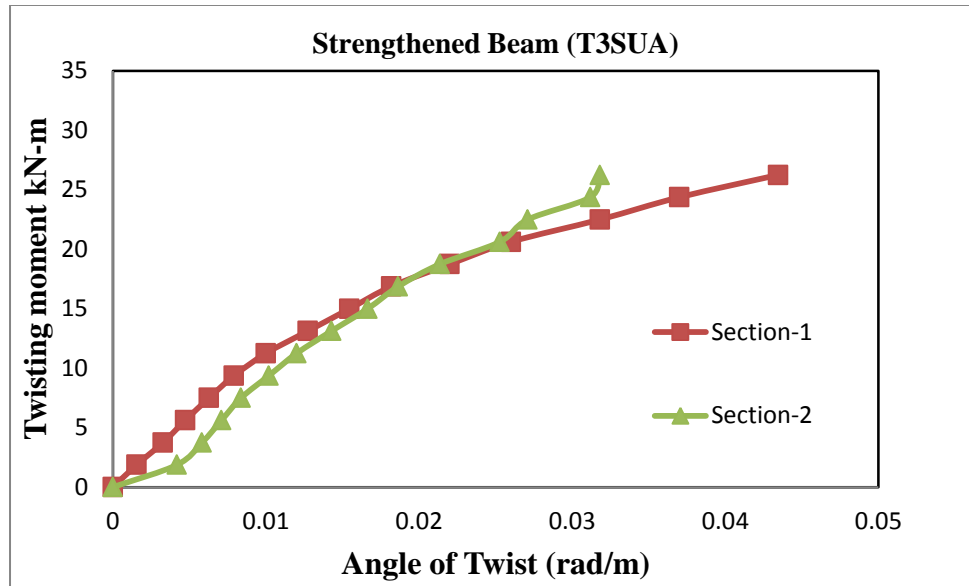


Fig 4.10 Torsional moment Vs Angle of Twist curve (T3SUA)

4.3.1.6 BEAM (T3SF)

Beam fully wrapped with 100mm strips of GFRP making 90° with longitudinal axis of the beam. The spacing of strip was maintained as 175 mm c/c. This beam is also tested till complete failure. The cracking pattern were same as the previous beams.



Fig 4.11(a) Fully Wrapped beam after Cracking



Fig 4.11(b) Cracks on Flange of Beam



Fig 4.11(c) Closed view of Cracks

Beam T3SF is taken as the strengthened beam for the series-B. In this Beam strengthening was done by full wrapping. At the load of 210 kN initial hairline cracks appeared. Later with the increase in loading values the crack propagated further. It has failed completely in torsion at a load 230kN and torsional moment 43.13 kNm. Increase strength of beam was 98.27% as the control beam. It was observed those cracks were initially generated in the web. And those cracks were appeared making an approximate angle 50° with the axis of main beam debonding was occurred when the beam reaches to ultimate load. The rupture of FRP was occurred and cracks were developed in a spiral pattern all over the main beam.

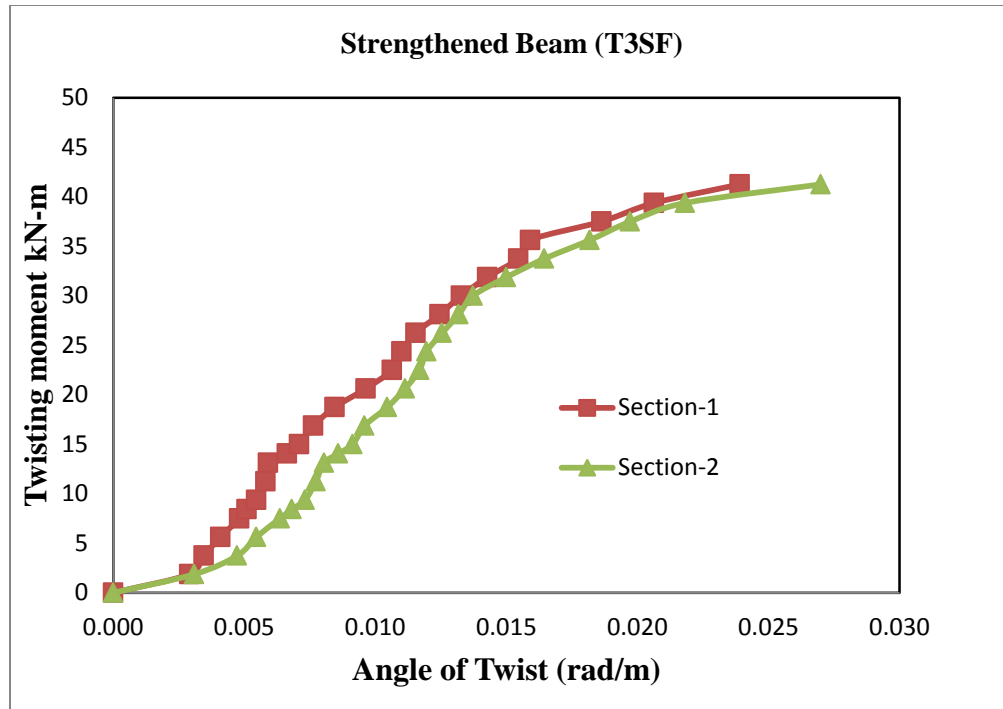


Fig 4.12 Torsional moment Vs Angle of Twist curve (T3SF)

4.3.1.7 BEAM NO (T3S45)



Fig 4.13(a) Beam wrapped with 100mm Bi-directional GFRP (45°) after cracking.



Fig.4.13 (b) Closed view of cracks



Fig.4.13 (c) crack in the flange

Beam T3S45 was strengthened by wrapping with four layers of 100mm wide bidirectional GFRP strips at a clear spacing of 75mm. The GFRP strips were wrapped over the beam by making an angle 45° with the main beam. At the load of 190 kN first cracking sound was heard. The Beam T3S45 failed completely in torsion at a load 210kN and torsional moment 39.37 kNm. The increase strength of beam was 81.03% as compared to control beam. The cracks were appeared making an angle 55° with the main beam on the side faces and 40° at the top surface. The FRP rupture has occurred in the torsion zone of main beam.

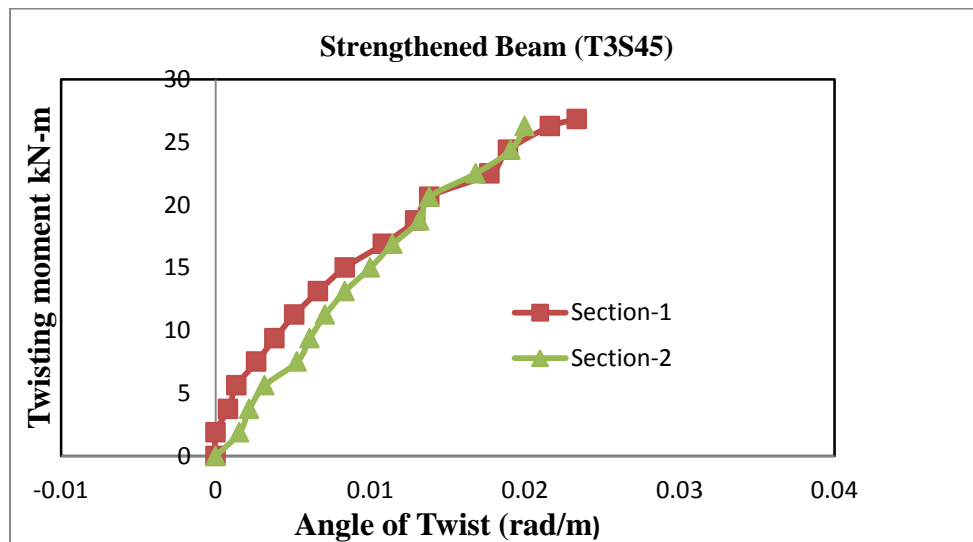


Fig 4.14 Torsional moment Vs Angle of Twist curve (T3S45)

4.3.1.8 BEAM (T4C)

Beam T4C is flanged RC beam with 450 mm wide flange. This beam was cast and tested to study effect of flange width on torsional behavior of T-Beam. In various design Codes a flange RC beam is designed like rectangular beam for torsion assuming that the shear flow takes place around the stirrups provided in the web portion only. The contribution of flange area in resisting torsional moment is neglected.



Fig 4.15(a) Crack pattern at face-1



Fig 4.15(b) Crack pattern at face-2

At the load of 120 KN initial hairline cracks appeared. Later with the increase in loading values the crack propagated further. The Beam failed completely in torsion at a load 152KN and torsional moment 28.5KNm. It was observed those cracks were appeared making an angle 40°-50° with the main beam. The cracks were developed in a spiral pattern all over the main beam which later leads to the collapse of the beam in torsional shear.

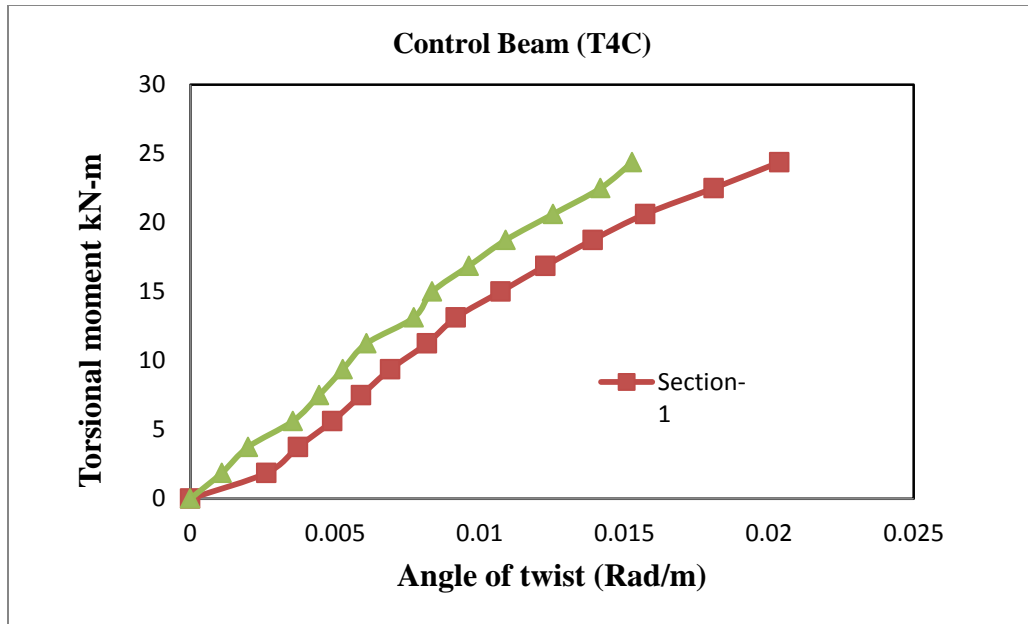


Fig 4.16 Torsional moment Vs Angle of Twist curve (T3C)

4.3.1.9 BEAM (T4SU)



Fig.4.17 (a) Beam 450mm flange strengthened with GFRP (U-Wrap)



Fig 4.17(b) Crack pattern at the main beam



Fig 4.17(c) Cracks in the flange portion.

The Beam T4SU was strengthened with four layers of bi-directional GFRP strips having U-wrap for web and bottom of the flange. The strips were 100 mm wide and applied @ 175 mm center to center. At the load of 160 kN initial hairline diagonal cracks appeared on flange as shown in the Fig.4.7b. With the increase of load diagonal cracks appeared in the concrete between the FRP strips making approximately. This is because strips acted like external reinforcement. Further increasing the load FRP debonding takes place at the ultimate load 208 kN and torsional moment 26.81 kNm. T3SU resulted in a 36.84% increase in torsional capacity over the control beam. It was observed that cracks were appeared making an angle 55° with the axis of main beam. The debonding of FRP were occurred and cracks were developed in a spiral pattern all over the main beam which later leads to the collapse of the beam in torsional shear.

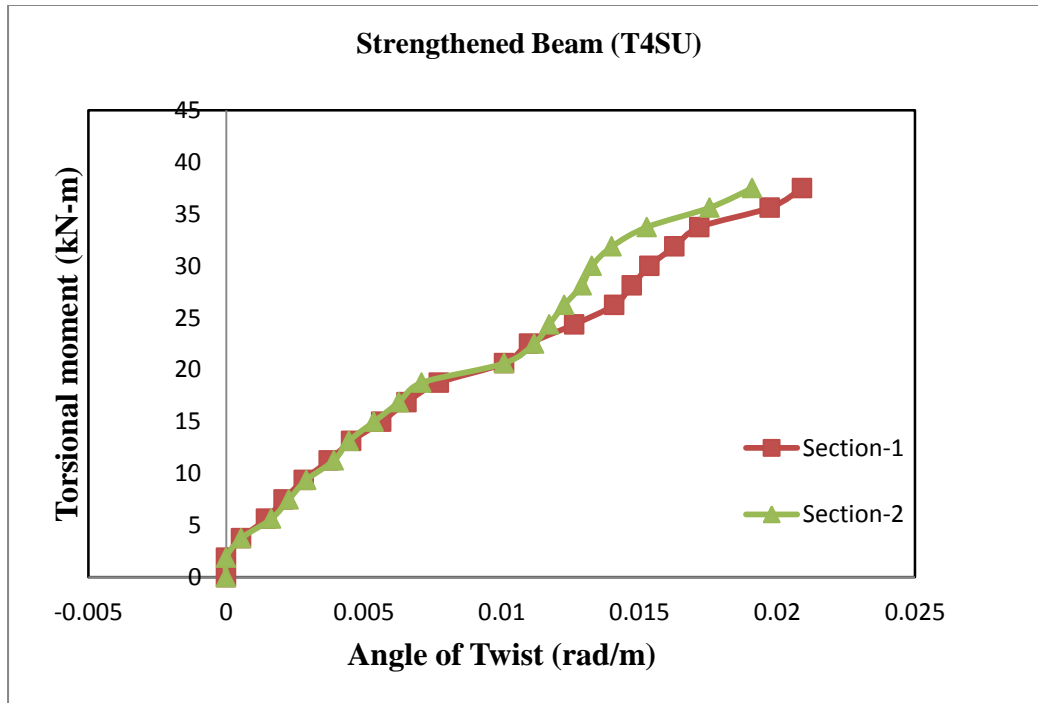


Fig 4.18 Torsional moment Vs Angle of Twist curve (T4SU)

4.3.1.10 BEAM (T3SUA)



Fig.4.19 (a) a closed view of crack



Fig.4.19 (b) Crack in web portion

The Beam T4SUA was strengthened with four layers of bi-directional GFRP strips of 100 mm width @ 175 mm c/c having U-wrap for web and bottom of the flange, and top of the flange. The FRP were not applied on vertical sides of the flange. This causes discontinuity to the shear flow along FRP. One anchor bolt is used on each sides of the flange and on each strip of FRP .Anchor threaded bolts carry axial tension force as a part of the shear flow resisting mechanism developed to resist the applied torsion. At the load of 210 kN initial hairline cracks appeared. Later with the increase in loading values the crack propagated further. It has failed completely in torsion at a load 240kN and torsional moment 46.13 KNm. The increase strength of beam was 61.84%as the control beam. It was observed those cracks were initially generated in the flange. The fig.4.21b shows rupture of FRP was occurred and cracks were developed in a spiral pattern all over the main beam. The cracks were generated making an approximate angle of 42°.

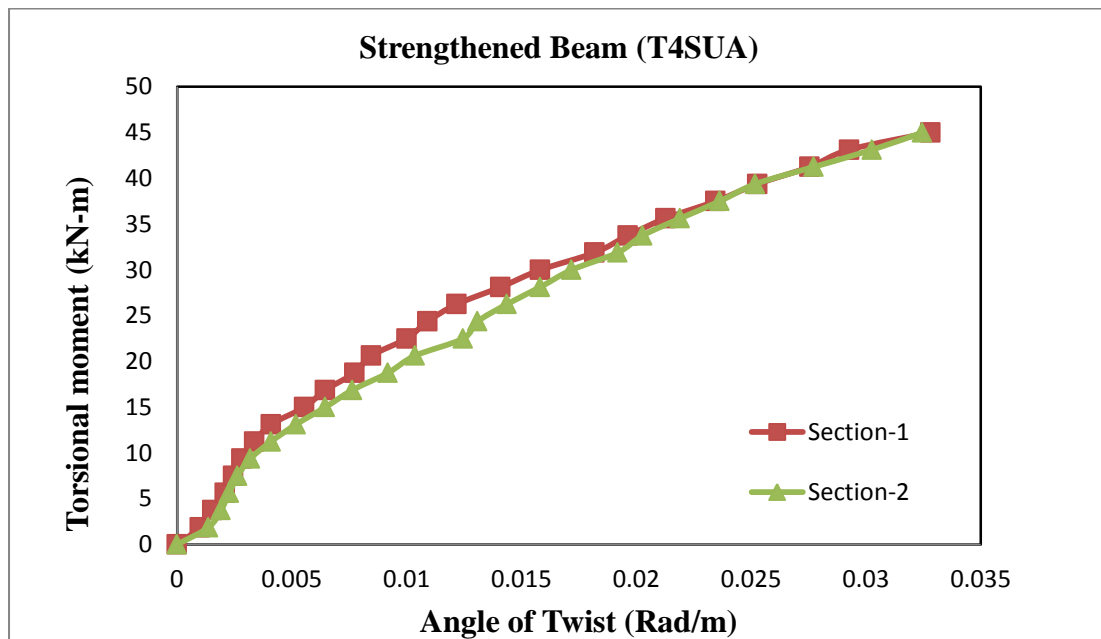


Fig 4.20 Torsional moment Vs Angle of Twist curve (T4SUA)

4.3.1.11 BEAM (T3SF)

Beam fully wrapped with 100mm strips of GFRP making 90° with longitudinal axis of the beam. The spacing of strip was maintained as 175 mm c/c. This beam is also tested till complete failure. The cracking pattern were same as the previous beams. Beam T4SF is taken as the strengthened beam for the series-B. In this Beam strengthening was done by full wrapping. At the load of 260 kN initial hairline cracks appeared. Later with the increase in loading values the crack propagated further. It has failed completely in torsion at a load 315kN and torsional moment 59.06 kNm. Increase strength of beam was 107.23% as the control beam. It was observed those cracks were initially generated in the web between the fiber strips . These cracks were appeared making an angle 50° with the axis of main beam was occurred when the beam reaches to ultimate load. The rupture of FRP was occurred and cracks were developed in a spiral pattern all over the main beam.



Fig 4.21(a) Fully Wrapped beam after Cracking of 450mm wide flange



Fig.4.21 (b) Debonding of FRP in web



Fig.4.21(c) cracks in flange

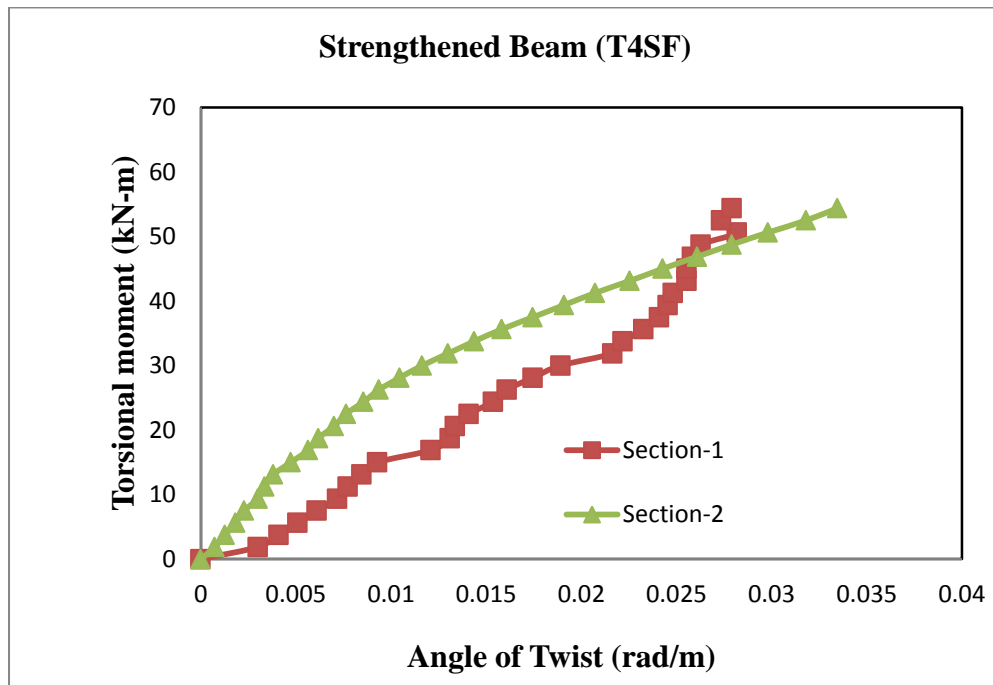


Fig 4.22 Torsional moment Vs Angle of Twist curve (T4SF)

4.3.1.12 BEAM (T3S45)

Beam T4S45 was strengthened by wrapping with four 100mm Bidirectional GFRP strips at a distance 75mm from each other over the beam. The GFRP strips were wrapped over the beam by making an angle 45° with the main beam. Using the loads and deflection data from experiment. At the load of 230KN cracking sound was heard. The Beam T4S45 failed completely in torsion at a load 297KN and torsional moment 56.25 KNm. The increase strength of beam was 95.33% as compared to control beam. The cracks were appeared making an angle 52° with the main beam on the side faces and 41° at the top surface. The FRP rupture has occurred in the torsion zone of main beam.



Fig.4.23(a) cracks in the web portion for 45° wrapping



Fig4.23(b) Debonding of FRP near the loading arms

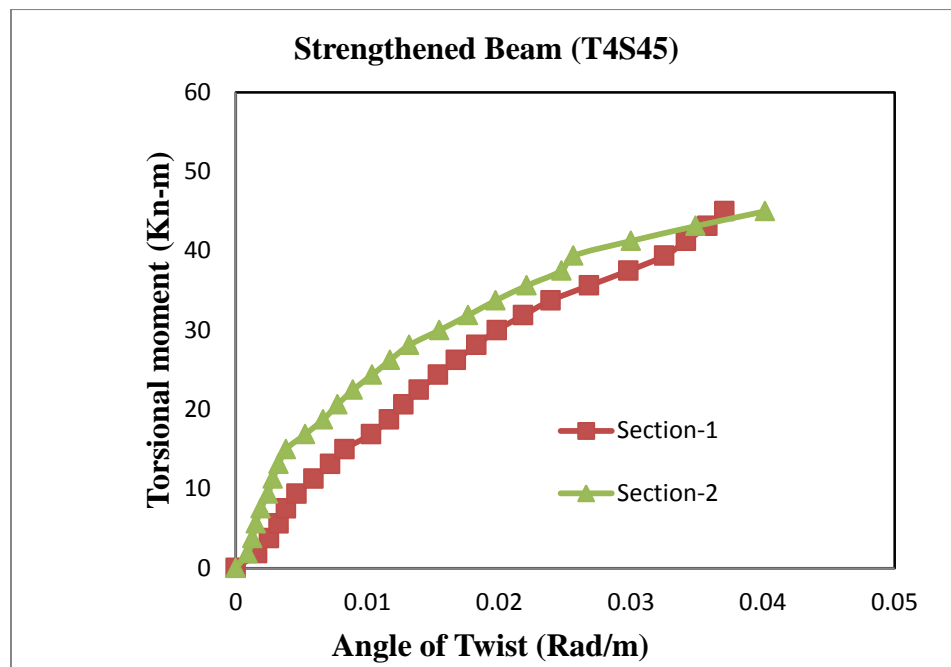


Fig 4.24 Torsional moment Vs Angle of Twist curve (T4S45)

4.4 Torsional Moment vs. Angle of Twist Curves

In this experiment load was applied on the two moment arm of the beams which is 0.35m away from the main beam and at the each increment of the load, deflection at $L/3$, $L/2$ and $2L/3$ is

taken with the help of dial gauges. Using this load and deflection data, the corresponding torsion moment and the twisting angle were calculated and the above graph was plotted.

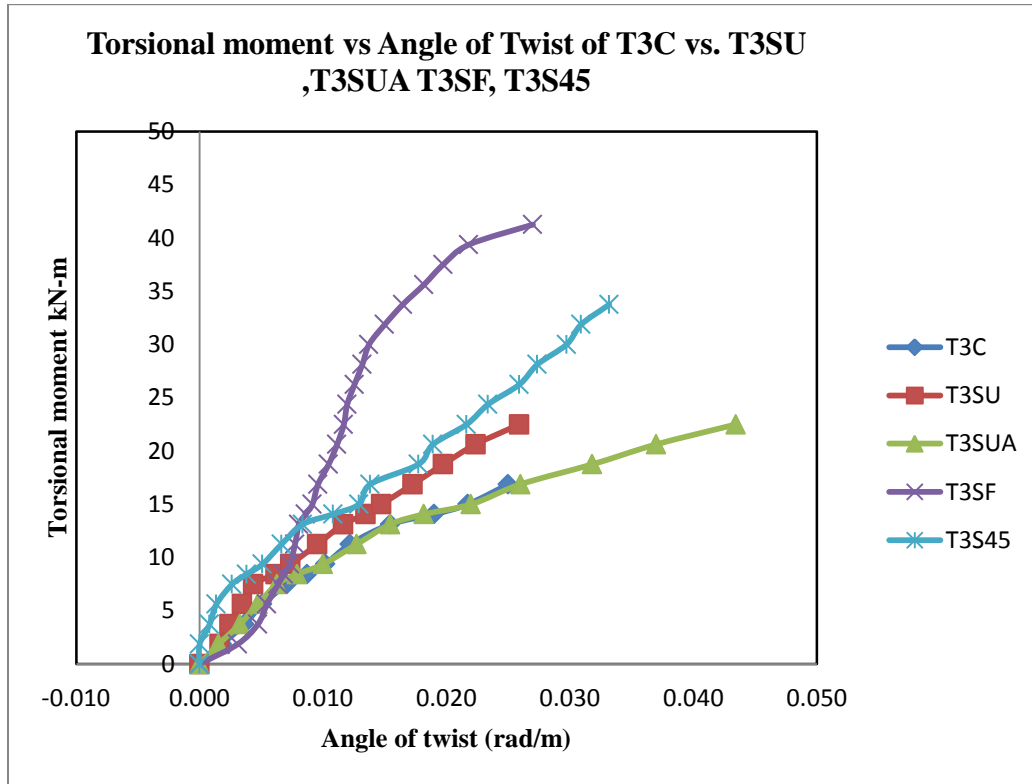


Fig.25 Effect of GFRP Strengthened patterns for Series B beams

From the above fig. we can conclude that fully wrapped pattern of GFRP (T3SF) strengthen provides maximum torsional strength and the 90-degree complete wrapping scheme provided an efficient confinement and in turn a significant increase in ultimate strength was observed, The increase in strength was 98.27% as compared with the control beam (T3C). Fully wrapped with 45° oriented fabric T3S45 also showed increase in ultimate strength of 81.03% as compared with T3C the reference beam.

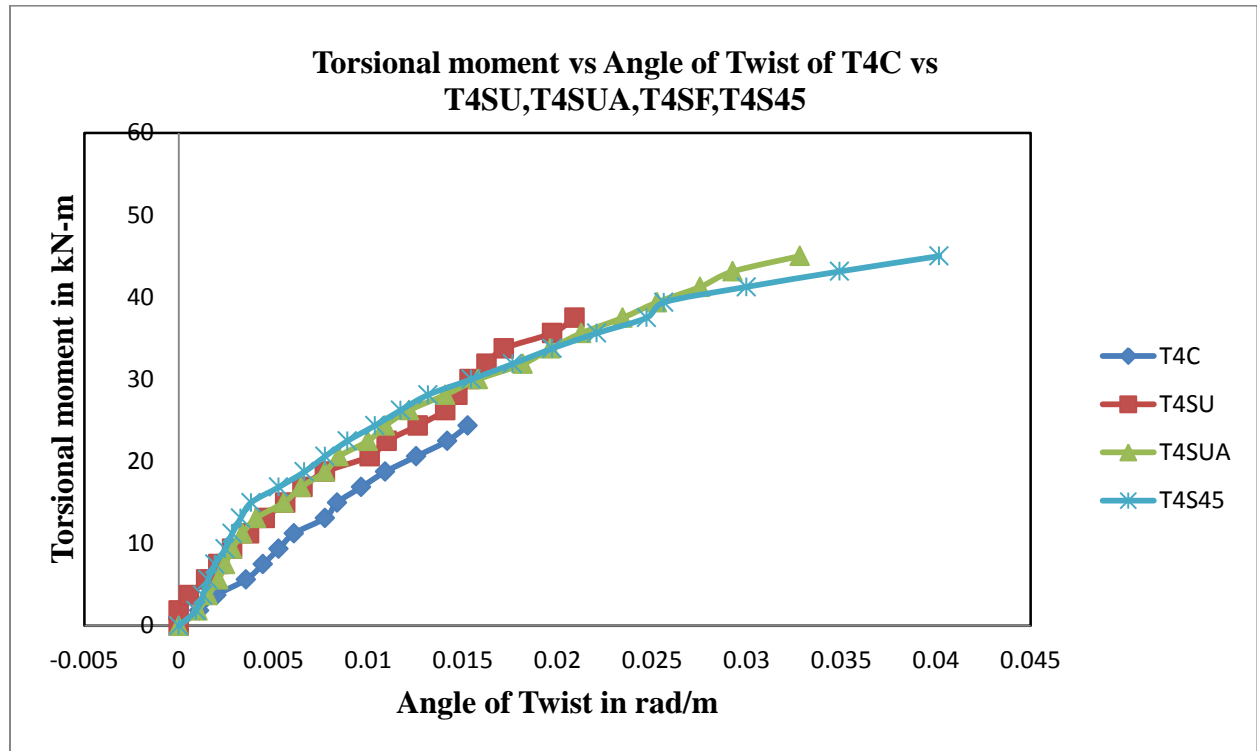


Fig.26 Effect of GFRP Strengthened patterns for Series C beams

In this group also the maximum ultimate strength was contributed by fully wrapped pattern of GFRP (T4SF). And complete wrapping scheme provided an efficient confinement and in turn a significant increase in ultimate strength was observed, the increase in strength was 107.23% as compared with the control beam (T4C). T4S45 also giving the increase in ultimate strength of 95.39% as compared with T4C.

The U-wrapped beam T4SU showed increase in ultimate strength by 36.84 % with respect to control beam T4C whereas the beam with anchor bolts T4SUA showed 61.83% increase in ultimate strength. The bolts provide continuity to shear flow path hence more capacity to resist the torsion. The beam T4SUA indicated more ductile behavior compared with T4SU.

All beams failed due to debonding. The beams with 45^0 -orientation exhibited fracture of fibers near major developed cracks after complete collapse. But the failure is basically due to debonding .

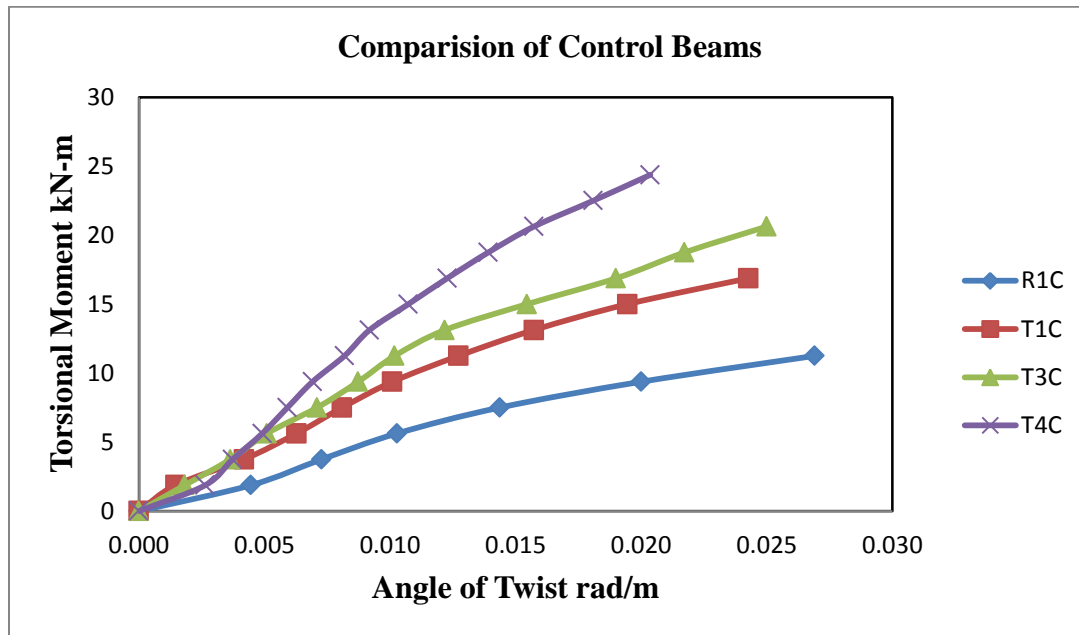


fig.27 Effect of flange width in control beams

In this graphs the significant increase of ultimate strength were increased by providing flanges. Effect of flange in torsional resisting was increased by increasing the width of flange. Various codes neglects the flange area of T-beam and consider only web area while calculating torsional capacity unless stirrups are provided in the flange area. The present study showed that unreinforced flange also contributes to the torsional capacity hence conventions given in the codes are on conservative side.

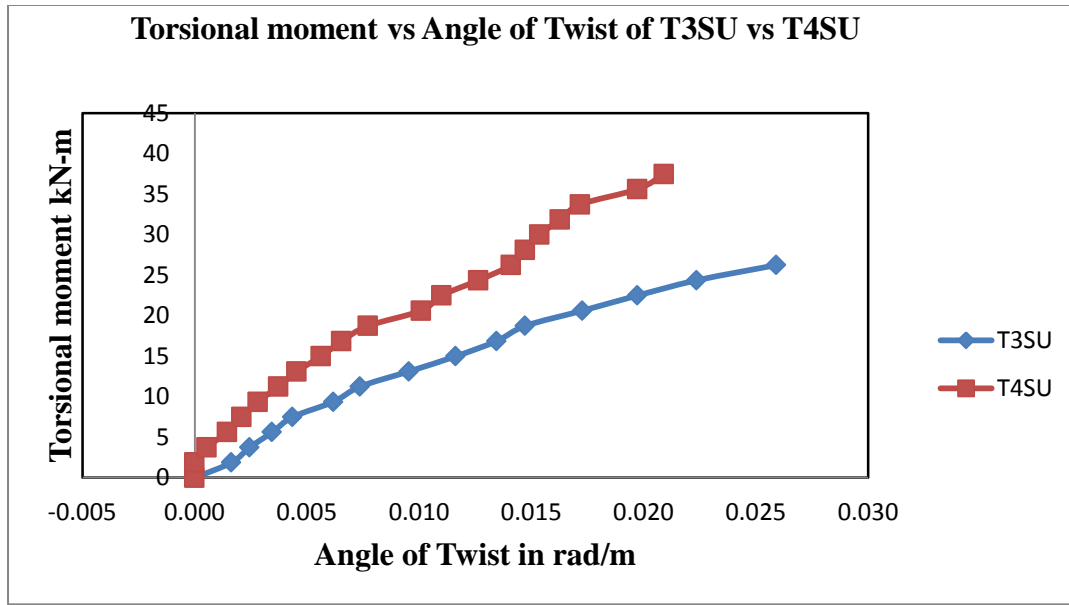


fig.28 Effect of GFRP Strengthened patterns for T3SU vs T4SU beams

T3SU and T4SU, beams expected that the strengthening scheme might not be efficient in improving the ultimate torsional strength when compared with the T3SF and T4SF. And it has given more ultimate strength compared to the control beams

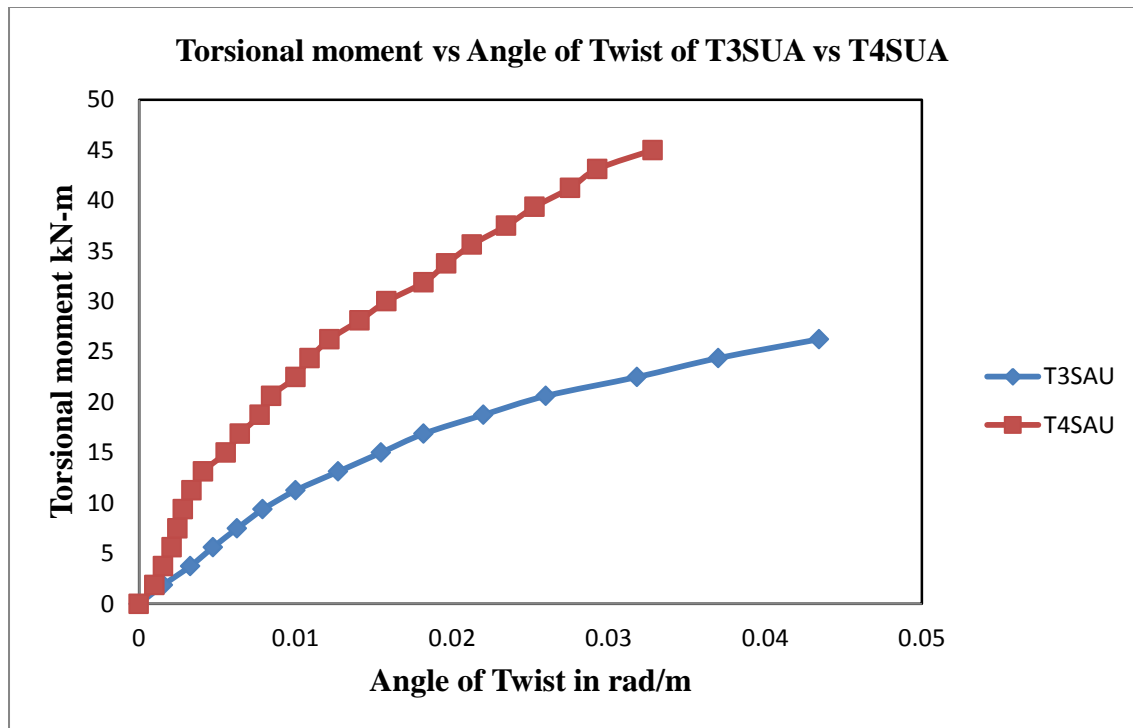


Fig.29 Effect of GFRP Strengthened patterns for T3SUA vs T4SUA beams

CHAPTER-5

ANALYTICAL ANALYSIS

CHAPTER 5

ANALYTICAL ANALYSIS

Various analytical models have been proposed for evaluating ultimate torque of FRP Strengthened Reinforced concrete beams. Earlier the FIB model introduced in 2001 was the only available analytical method to evaluate the FRP contribution in the ultimate torsional capacity of the RC beams. This contribution for fully wrapped and U-wrapped beams are given as

$$T_{uf} = 2bh \frac{t_f b_f \epsilon_{fe} E_f w_f}{s_f} \cot \Theta \text{ for fully wrapped RC beams}$$

$$T_{uf} = bh \frac{t_f b_f \epsilon_{fe} E_f w_f}{s_f} \cot \Theta \text{ for U wrapped RC beams}$$

where Θ =angle of torsion crack measured from the member's longitudinal axis;

ϵ_{fe} =effective strain in the fibers to be obtained using the recommendations of FIB (2001);

b and h= cross-sectional dimensions of the beam;

b_f =width of FRP;

E_f =modulus of elasticity of FRP; and

s_f =spacing of the FRP strips.

This model did not include the distribution of stresses among the concrete, reinforcement and FRP, hence produces erroneous results.

This model was further modified including the interaction between these elements by many researchers and presented in various papers.

The model used for validation of the experimental results of present study are developed by A.Deifalla and A. Ghobarah¹⁵ is a simplified procedure to evaluate FRP contribution to torsional capacity of RC beams.

They proposed that FRP contribution to the total torsion capacity can be calculated by

$$T_f = \frac{2 A_o f_f A_f [\cot \beta + \cot \Theta] \sin \beta}{S_f}$$

A_o = area enclosed inside the critical shear flow path due to strengthening

f_f = stress in the FRP sheet at failure,

β = angle of orientation of the fiber direction to the longitudinal axis of the beam,

S_f = spacing between the centerline of the FRP strips,

A_f = effective area of the FRP resisting torsion calculated by

$$A_f = n t_f w_f$$

w_f = width of FRP strips

Where n = number of FRP strips,

$$f_f = E_f \epsilon_{fe}$$

Where ϵ_{fe} = effective strain in fibres calculated by

$$\epsilon_{fe} = \frac{0.33 w_f}{L_e S_f} \text{ for debonding failure of FRP}$$

Where L_e = effective bond length calculated by

$$L_e = \sqrt{\frac{E_f t_f}{\sqrt{f_c}}}$$

Where f_c = compressive strength of concrete

Following the above equations and using material properties and specimen dimensions the torsional resistance provided by the FRP for beams are calculated and given in Table.

GFRP properties $E_f = 9493 \text{ N/mm}^2$

Table 5.1 Comparison of Analytical and Experimental Results

Beam Name		t_f (mm)	n	θ	B	f_c N/mm^2	$T_{f,cal}$ kN m	$T_{fexp} =$ $T_{ult*} - T_{cont*}$ kNm	$\frac{T_{f,cal}}{T_{fexp}}$
Series- A	T3SU	2.26	5	65°	90°	28.62	28.61	27	1.05
	T3SF	2.51	5	50°	90°	28.69	109.61	114	0.96
	T3S45	2.46	4	55°	45°	28.69	99.69	94	1.060
Series- B	T4SU	2.43	5	55°	90°	30.89	51.3	56	0.91
	T4SF	2.53	5	45°	90°	30.77	149.98	163	0.97
	T4S45	2.28	4	42°	45°	29.83	133.17	145	0.91

* T_{ult} - ultimate torsional moment of FRP strengthen beam,

* T_{cont} - ultimate torsional moment of control beam.

The calculated values compares well with the experimental values.

CHAPTER – 6

CONCLUSIONS

CHAPTER-6

CONCLUSIONS

The experimental program of this study consists of eleven numbers of reinforced concrete T- beams with different flange widths tested under torsion. The main objective of this study is to investigate the effectiveness of the use of epoxy-bonded FRP fabrics as external transverse reinforcement. Based on presented experimental measurements and analytical predictions, the following conclusions were reached

- Experimental results shows that the effect of flange width on torsional capacity of GFRP strengthened RC T-beams are significant.
- Torsional strength increases with increase in flange area irrespective of beam strengthening with GFRP following different configurations schemes.
- With 250 mm wide flange width increase in strength was 13%, with 350mm wide flange was 29% and for 450mm wide flange was found to be 69%. This is due to increase in area enclosed inside the critical shear path.
- The cracking and ultimate torque of all strengthen beams were greater than those of the control beams.
- The increase in magnitude depends on the FRP strengthening configurations.
- The maximum increase in torque was obtained for 90⁰ fully wrapped configurations. Increase of 133.33% to 116.67% in first cracking and 155.55% to 107.23% in ultimate torsion were recorded for series B beams and series C beams respectively.
- Beams fully wrapped with 45⁰ oriented GFRP stripes showed next highest torsional resisting capacity. Increase of 111.11% to 91.667% in first cracking and 81.03% to

95.39% in ultimate torsion were recorded for series B beams and series C beams respectively.

- Beams U wrapped with 90^0 oriented GFRP stripes showed lowest torsional resisting capacity. Since shear flow stresses take a close path during torsional loading ,torsion would not be well resisted in case of U-jacketing strengthening.
- For U wrapped beams increase of 22.22% to 33.33% in first cracking and 23.27% to 36.84% in ultimate torsion were recorded for series B beams and series C beams respectively.
- Beams strengthen with U jacketing in web and top of flange and anchored with bolts exhibited increase of 11.11% to 55% in first cracking and 28.33% to 61.84% in ultimate torsion were recorded for series B beams and series C beams respectively.
- The torsional resisting capacity of these beams was found to be more than beams strengthen with U jacketing only. In such beams anchor bolts carry axial tensile forces as a part of shear flow resisting mechanism developed to resist the applied torsional moment.
- Strengthened beams using GFRP strips as the only transverse reinforcement exhibited better overall torsional performance than the non-strengthened control beams.
- The use of continuous FRP strips that wrapped around the cross-section of T-beams caused a significant increase on the ultimate torsional strength. It is concluded that full wrapping with continuous strips is far more efficient for torsional upgrading than the use of wrapping with the discrete strips.
- Although the extended FRP U-jacket strengthening technique relatively less effective than the FRP full wrapping strengthening technique, it yielded promising results in terms

of strength and ductility while being quite feasible for most strengthening practical situations.

- The experimental results were validated with simplified model proposed by A. Deifalla & A. Ghobarah¹⁵. The model included the effect of different parameters studied in the present work like strengthening techniques, thickness and number of layers, spacing between FRP strips, FRP orientations, and angle of diagonal cracks.
- Experimental results indicate that the estimation of the GFRP contribution to torsional strength using simplified model proposed by A. Deifalla & A. Ghobarah provided good accuracy for GFRP strengthen beams.

CHAPTER – 7

REFERENCES

REFERENCES

1. ACI Committee 440 (1996) State Of Art Report On Fiber Reinforced Plastic
2. Ameli, M. and Ronagh, H.R. (2007). "Behavior of FRP strengthened reinforced concrete beams under torsion", *Journal of Composites for Construction*, 11(2), 192-200.
3. Ameli, M., and Ronagh, H. R. (2007), "Analytical method for evaluating ultimate torque of FRP strengthened reinforced concrete beams" ,*Journal of Composites for Construction* ,11, 384–390.
4. Amir, M., Patel, K. (2002). "Flexural strengthening of reinforced concrete flanged beams with composite laminates", *Journal of Composites for Construction*, 6(2), 97-103.
5. Andre, P., Massicotte, Bruno, Eric, (1995). "Strengthening of reinforced concrete beams with composite materials : Theoretical study", *Journal of composite Structures*,33,63-75
6. Arbesman, B. (1975). "Effect of stirrup cover and amount of reinforcement on shear capacity of reinforced concrete beams." MEng thesis, Univ. of Toronto.
7. Arduini, M., Tommaso, D. A., Nanni, A. (1997), "Brittle Failure in FRP Plate and Sheet Bonded Beams", *ACI Structural Journal*, 94 (4), 363-370.
8. Belarbi, A., and Hsu, T. T. C. (1995). "Constitutive laws of softened concrete in biaxial tension-compression." *ACI Structural Journal*, 92, 562-573.
9. Chalioris, C.E. (2006). "Experimental study of the torsion of reinforced concrete members", *Structural Engineering & Mechanics*, 23(6), 713-737.

10. Chalioris, C.E. (2007a). “Torsional strengthening of rectangular and flanged beams using carbon fibre reinforced polymers – Experimental study”, *Construction & Building Materials*, in press (available online since 16 Nov. 2006).
11. Chalioris, C.E. (2007b). “Tests and analysis of reinforced concrete beams under torsion retrofitted with FRP strips”, *Proceedings 13th Computational Methods and Experimental Measurements (CMEM 2007)*, Prague, Czech Republic.
12. Chen, J.F. and Teng, J.G. (2003a). “Shear capacity of fiber-reinforced polymer-strengthened reinforced concrete beams: Fiber reinforced polymer rupture”, *Journal of Structural Engineering*, ASCE, 129(5), 615-625.
13. Chen, J.F. and Teng, J.G. (2003b). “Shear capacity of FRP-strengthened RC beams: FRP debonding”, *Construction & Building Materials*, 17, 27-41.
14. Deifalla A. and Ghobarah A.(2010), “Full Torsional Behavior of RC Beams Wrapped with FRP: Analytical Model”, *Journal of Composites for Construction*,14,289-300.
15. A. Deifalla and A. Ghobarah (2005) “Simplified analysis for Torsionaly Strengthened RC beams using FRP’*Proceedings of the International Symposium on Bond Behaviour of FRP in Structures (BBFS 2005)*
16. Gobarah,A., Ghorbel, M., and Chidiac, S. (2002). “Upgrading torsional resistance of RC beams using FRP.” *Journal of Composites for Construction* ,6,257–263.
17. Hii, A. K. Y., and Al-Mahadi, R. (2007). “Torsional capacity of CFRP strengthened reinforced concrete beams.” *Journal of Composites for Construction*,11,71–80.

18. Hii, A.K.Y. and Al-Mahaidi, R. (2006). "An experimental and numerical investigation on torsional strengthening of solid and box-section RC beams using CFRP laminates", *Journal of Composite Structures*, 75, 213-221.
19. Karayannis, C.G. and Chalioris, C.E. (2000a). "Experimental validation of smeared analysis for plain concrete in torsion", *Journal of Structural Engineering*, ASCE, 126(6), 646-653.
20. Karayannis, C.G. and Chalioris, C.E. (2000b). "Strength of prestressed concrete beams in torsion", *Structural Engineering & Mechanics*, 10(2), 165-180.
21. Mahmood, M. N. and Mahmood, A. Sh.(2011) "Torsional behaviour of prestressed concrete beam strengthened with CFRP sheets" 16th International Conference on Composite Structures, ICCS 16
22. Mitchell, D. and Collins, M. P. (1974). "Diagonal compression field theory-A rational model for structural concrete in pure torsion." *ACI Struct. J.*, 71, 396-408.
23. Onsongo, W. M. (1978). "Diagonal compression field theory for reinforced concrete beams subjected to combined torsion, flexure, and axial load." Ph.D. thesis, Univ. of Toronto, Toronto.
24. Panchacharam, S. and Belarbi, A. (2002). "Torsional behaviour of reinforced concrete beams strengthened with FRP composites", *Proceedings 1st FIB Congress*, Osaka, Japan, 1-10.
25. Pham, H. B., and Al-Mahaidi, R. (2004). "Experimental Investigations into flexural retrofitting of reinforced concrete beams using fiber reinforced polymer." *J. Compos. Constr.*, 6(4), 257-263.

26. Rahal, K. N., and Collins, M. P. (1995). "Effect of the thickness of concrete cover on the shear-torsion interaction—An experimental investigation." *ACI Struct. J.*, 92, 334–342.
- Reinforcement For Concrete Structure , ACI 440R-96, American Concrete Institute , Farmington Hills, Michigan
27. Salom, P.R., Gergely, J.M. and Young, D.T. "Torsional strengthening of spandrel beams with fiber-reinforced polymer laminates", *Journal of Composites for Construction*, 8(2), 157-162.
28. Tastani, S.P. and Pantazopoulou, S.J. (2004). "Experimental evaluation of FRP jackets in upgrading RC corroded columns with substandard detailing", *Engineering Structures*, 26, 817
29. Teng, J. G., Chen, J. F., Smith, S. T., and Lam, L. (2002). *FRP strengthened RC structures*, Wiley, Chichester, U.K.
30. Triantafillou, T.C. and Antonopoulos, C.P. (2000). "Design of concrete flexural members strengthened in shear with FRP", *Journal of Composites for Construction*, 4(4), 198-205.
31. Zhang, J. W., Lu, T. Z., and Zhu, H. (2001). "Experimental study on the behavior of RC torsional members externally bonded with CFRP". *FRP composites in civil engineering*, I, Elsevier Science, New York.
32. Zojaji A.R. and Kabir M.Z. (2011) "Analytical approach for predicting full torsional behavior of reinforced concrete beams strengthened with FRP materials". *Scientia Iranica A*.19 (1), 51–63.